AD-A176 952 INSTRUMENTATION FOR PICOSECOND OPTICAL ELECTRONICS RESEARCH(U) STANFORD UNIV CA EDWARD L GINZTON LAB OF PHYSICS D M BLOOM MAY 86 AFOSR-85-0165 1/1

UNCLASSIFIED F/G 9/5 NL

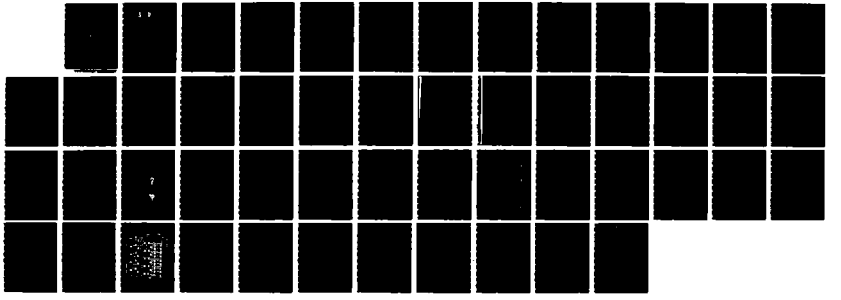

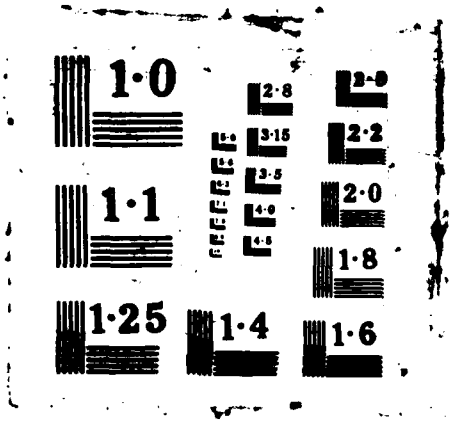
1·0
1·1
1·25
1·4
1·6
2·8
3·15
3·5
2·0
2·2
2·0
1·8

(2)

UNCLASSIFIED

SECURITY CLASSIFICATION OF THIS PAGE

REPORT DOCUMENTATION PAGE

1a. REPORT SECURITY CLASSIFICATION Unclassified	1b. RESTRICTIVE MARKINGS
2a. SECURITY CLASSIFICATION AUTHORITY	3. DISTRIBUTION/AVAILABILITY OF REPORT Approved for public release; Distribution unlimited
2b. DECLASSIFICATION/DOWNGRADING SCHEDULE	
4. PERFORMING ORGANIZATION REPORT NUMBER(S)	5. MONITORING ORGANIZATION REPORT NUMBER(S) AFOSR-TR- 87-0174
6a. NAME OF PERFORMING ORGANIZATION Edward L. Ginzton Laboratory Stanford University	6b. OFFICE SYMBOL (If applicable)
	7a. NAME OF MONITORING ORGANIZATION AFOSR/NP
6c. ADDRESS (City, State and ZIP Code) Edward L. Ginzton Laboratory W.W. Hansen Laboratories of Physics Stanford University, Stanford CA 94305	7b. ADDRESS (City, State and ZIP Code) Bldg 410 Bolling AFB, D.C. 20332-6448
8a. NAME OF FUNDING/SPONSORING ORGANIZATION AFOSR	8b. OFFICE SYMBOL (If applicable) NP
	9. PROCUREMENT INSTRUMENT IDENTIFICATION NUMBER AFOSR 85-0165
8c. ADDRESS (City, State and ZIP Code) SAME AS 7B.	10. SOURCE OF FUNDING NOS.

PROGRAM ELEMENT NO.	PROJECT NO.	TASK NO.	WORK UNIT NO.
61102F	2301	A1	

11. TITLE (Include Security Classification)
"INSTRUMENTATION FOR PICOSECOND OPTICAL ELECTRONICS RESEARCH", (U)

12. PERSONAL AUTHOR(S)
DR D M BLOOM

13a. TYPE OF REPORT	13b. TIME COVERED	14. DATE OF REPORT (Yr., Mo., Day)	15. PAGE COUNT
FINAL	FROM 85/03/15 TO 86/03/14	May 1986	49

16. SUPPLEMENTARY NOTATION

17. COSATI CODES			18. SUBJECT TERMS (Continue on reverse if necessary and identify by block number)
FIELD	GROUP	SUB. GR.	Optics, picosecond, Electrooptics

19. ABSTRACT (Continue on reverse if necessary and identify by block number)

An electrooptic (EO) sampling system for high-speed measurements on galium arsenide (GaAs) integrated circuits (IC's) was developed. This measurement technique is based on the linear electrooptic effect in GaAs. Using longitudinal probing geometry, sub-bandgap energy infrared light is passed through the substrate of a GaAs IC, reflected off some circuit metallization, and passed through a polarizer, resulting in an intensity of change of the light past the polarizer proportional to the voltage across the substate. To achieve short temporal resolution, the signal generating electronics for driving the IC's are phase locked to the repetition rate of a mode-locked laser system to allow for repetitively sampled measurements of time waveforms. Since the probe is an optical beam, the technique is non-contact, non-destructive, and non-invasive in that the test point is not leaded with 50 ohms ar any parasitic impedences.

20. DISTRIBUTION/AVAILABILITY OF ABSTRACT	21. ABSTRACT SECURITY CLASSIFICATION
UNCLASSIFIED/UNLIMITED ☒ SAME AS RPT. ☒ DTIC USERS ☐	UNCLASSIFIED

22a. NAME OF RESPONSIBLE INDIVIDUAL	22b. TELEPHONE NUMBER (Include Area Code)	22c. OFFICE SYMBOL
HOWARD R. SCHLOSSBERG	(202)767-4906	NP

DD FORM 1473, 83 APR EDITION OF 1 JAN 73 IS OBSOLETE.

UNCLASSIFIED

SECURITY CLASSIFICATION OF THIS PAGE

Edward L. Ginzton Laboratory
W. W. Hansen Laboratories of Physics
Stanford University
Stanford, California 94305

Final Report
Air Force Office of Scientific Research
on
The Program of Research
"Instrumentation for
Picoscond Optical Electronics Research"
Grant # AFOSR-85-0165
Covering Period: March, 15, 1985 to March 14, 1986

Principal Investigator:
D. M. Bloom
Associate Professor of Electrical Engineering

May 1986

Table of Contents

A Program of Research in Picosecond Optical Electronics

I. Summary

An electrooptic (EO) sampling system suitable for high-speed measurements on gallium arsenide (GaAs) integrated circuits (IC's) was developed. This measurement technique is based on the linear electrooptic effect in GaAs. Using a longitudinal probing geometry, sub-bandgap energy infrared light is passed through the substrate of a GaAs IC, reflected off some circuit metallization, and passed through a polarizer, resulting in an intensity change of the light past the polarizer proportional to the voltage across the substrate. To achieve short temporal resolution, the signal generating electronics for driving the IC's are phase locked to the repetition rate of a mode-locked laser system to allow for repetitively sampled measurements of time waveforms. Since the probe is an optical beam, the technique is non-contact, non-destructive, and non-invasive in that the test point is not loaded with 50 ohms or any parasitic impedences. For analog circuits, the sampler can be used in the small-signal case to make vector voltage measurements or in the large signal case to view distortion and clipping of time waveforms. For digital circuits, the sampler can be used to measure signal timing, risetimes of less than 10 picoseconds (ps), and propagation delays to 1 ps.

II. Research Results

The results of this research are well documented in the literature (see attached publications list and appendix). A summary of these results in chronological order are given below.

During the summer of 1984 the initial version of the electrooptic sampler was developed. The system consisted of mode-locked Nd:YAG laser, a fiber-grating pulse compressor, a doubling crystal for second-harmonic generation, an optical breadboard with the

necessary optics, a stepper motor stage, viewing system, a photodiode receiver, and a desk-top computer controller. The system was demonstrated by measuring the time response of a 30 ps GaAs photodiode by exciting the photodiode with the doubled light, launching the signal and a GaAs transmission, and measuring the response electrooptically using the infrared light. This work was completed by October 1984.

During the next several months, the ability to directly measure time waveforms from signal generators synchronized to the laser pulse repetition rate was investigated. The concept proved feasible but the laser was identified as a source of excess timing instability. Measuring the phase noise of the laser by harmonic mixing of the laser spectrum with a microwave synthesizer on a GaAs microstrip, the timing jitter of the laser was characterized [1]. This excess timing jitter seriously degraded sampling measurements of synthesizer signals above 10 GHz.

To combat this excess timing jitter, an electronic, phase-sensitive feedback loop external to the laser was developed. This system compared the timing of the pulses from the laser to a very stable signal from an RF synthesizer. Timing error on the laser pulses generated an error signal that controlled a phase-shifter to adjust the timing signal to the mode-locker of the laser. In this fashion, the timing jitter was substantially reduced. Improvements on this timing stabilizer continued through August 1985, with a resulting timing jitter of 2 picoseconds (ps) rms overall and a long term drift of less than 1 ps per minute of the laser pulses with respect to a microwave synthesizer signal.

Concurrently with the above effort, the electrooptic sampler was being applied to the characterization of GaAs integrated circuits (IC's). Working with a 2-12 GHz traveling-wave amplifier (TWA) from Varian Associates, vector measurements of internal node signals on this circuit were demonstrated as well as detection of signals to 26 GHz, the limit of the labs microwave synthesizer [2].

To apply this system to signal detection on digital circuits, a novel backside probe geometry was conceived and demonstrated [3]. A high-speed 8-bit multiplexer/demultiplexer from TriQuint Semiconductor was probed in this fashion, demonstrating the ability to

detect the signal timing and propagation delays logic elements along 2 micron width interconnects.

In conclusion, this contract supported research of a new type of electrooptic sampling that allows for synchronization of a microwave synthesizer with the pulse repetition rate of a mode-locked laser. With feedback electronics to stabilize the timing of the laser pulses, the response of analog and digital GaAs IC's can be detected with picosecond accuracy. This research has led to a number of publications [1] -[9] and the electrooptic sampler is becoming a valuable new tool for the accurate characterization of ultrafast GaAs integrated circuits.

III. Personnel

During the course of this project, two students were awarded degrees. Kurt Weingarten received his M.S. Degree in Electrical Engineering in April of 1985, and Brian Kolner received his Ph.D. in June of 1985. Dr. Kolner's thesis was entitled "Picosecond *Electro-optic Sampling* of Gallium Arsenide".

Appendix I.

Publications

Ultrafast Electronics Laboratory

E. L. Ginzton Laboratory

Stanford University

[1] B. H. Kolner, K. J. Weingarten, M. J. W. Rodwell and D. M. Bloom, "Picosecond Electrooptic Sampling and Harmonic Mixing in GaAs," *Picosecond Electronics and Optoelectronics,* G. A. Mourou, D. M. Bloom and C. H. Lee, eds. (New York: Springer-Verlag, 1985) pp. 50-53.

[2] K. J. Weingarten, M. J. Rodwell, H. K. Heinrich, B. H. Kolner and D. M. Bloom, "Direct Electro-optic Sampling of GaAs Integrated Circuits," Elect. Lett. **21**, 765-766 (August 1985).

[3] J. L. Freeman, S. K. Diamond, H. Fong and D. M. Bloom, "Electro-optic Sampling of Planar Digital GaAs Integrated Circuits," Appl. Phys. Lett. **47** (10), 1083-1084 (November 15, 1985).

[4] J. L. Freeman, K. J. Weingarten, M. J. W. Rodwell, S. K. Diamond, H. Fong and D. M. Bloom, "Direct Electro-optic Sampling of Analog and Digital GaAs Integrated Circuits," *GaAs IC Symposium* 147-150 (November 1985).

[5] K. J. Weingarten, M. J. W. Rodwell, J. L. Freeman, S. K. Diamond and D. M. Bloom, "Characterization of GaAs Integrated Circuits by Direct Electro-Optic Sampling," *International Electron Devices Meeting*, pp. 479-482 (December 1985).

[6] B. H. Kolner and D. M. Bloom, "Electro-optic Sampling in GaAs Integrated Circuits," IEEE J. Quantum Electron. vol. **QE-22** 79-93 (January 1986).

[7] M. J. W. Rodwell, K. J. Weingarten, J. L. Freeman and D. M. Bloom, "Gate Propagation Delay and Logic Timing of GaAs Integrated Circuits Measured by Electro-Optic Sampling," *submitted to Electronics Letters.*

[8] M. J. W. Rodwell, M. Riaziat, K. J. Weingarten, B. A. Auld and D. M. Bloom, "Internal Microwave Propagation and Distortion Characteristics of Travelling-Wave Amplifiers Studied by Electro-Optics Sampling," *To be published in the 1986 MTT Conference Journal.*

[9] K. J. Weingarten, M. J. W. Rodwell, J. L. Freeman, S. K. Diamond and D. M. Bloom, "Electrooptic Sampling of Gallium Arsenide Integrated Circuits," *Invited Paper to the Topical Meeting on Ultrafast Phenomena, 1986.*

Appendix II.

Oral Disclosures

May, 1985 - January, 1986

Stanford University

[1] "Electro-Optic Sampling of GaAs Integrated Circuits" AT&T Bell Laboratories, Holmdel, New Jersey, July 23, 1985. M. J. Rodwell.

[2] "Electro-Optic Sampling of GaAs Integrated Circuits" AT&T Bell Laboratories, Murray Hill, New Jersey, July 24, 1985. D. M. Bloom.

[3] "Electro-Optic Sampling of GaAs Integrated Circuits" IBM Yorktown Heights, Yorktown Heights, New York, July 25, 1985. D. M. Bloom.

[4] "Optical Detection Methods and Limits" Picosecond Electronics, UCSB Extension, Santa Barbara, California, August 15, 1985. D. M. Bloom.

[5] "Ultrafast Optical Electronics", LEOS Lecture Series, University of Texas, Dallas, Texas, September 25, 1985. D. M. Bloom.

[6] "Electro-Optic Sampling of GaAs Integrated Circuits", Texas Instruments, Dallas, Texas, September 26, 1985. D. M. Bloom.

[7] "Electro-Optic Sampling of Planar Digital GaAs Integrated Circuits", GaAs IC Symposium, Monterey, California, November 14, 1985. J. Freeman.

[8] "Electro-Optic Sampling of GaAs Integrated Circuits", Varian Associates, Palo Alto, California, November 18, 1985. M. J. Rodwell.

[9] "Direct Electro-Optic Sampling of GaAs Integrated Circuits", International Electron Devices Meeting, Washington, DC, December 4, 1985. K. Weingarten

Appendix III.

Reprints and Preprints

Picosecond Electrooptic Sampling and Harmonic Mixing in GaAs

B.H. Kolner, K.J. Weingarten, M.J.W. Rodwell, and D.M. Bloom
Edward L. Ginzton Laboratory, Stanford University,
Stanford, CA 94305, USA

Electro-optic sampling is a powerful technique for exploiting the capabilities of modern mode-locked laser systems to make high speed electronic measurements. Using ultrashort light pulses to probe the electric fields of microstrip transmission lines deposited on $LiNbO_3$ and $LiTaO_3$, VALDMANIS et al. [1,2] demonstrated an electro-optic sampling system capable of resolving picosecond and subpicosecond rise-time photoconductive switches. KOLNER et al. [4,5] utilized a similar system to characterize photodiodes exhibiting bandwidths of 100 GHz. In both cases, a hybrid connection between the device under test and the electro-optic transmission line was required. VALDMANIS et al. [6] and MEYER and MOUROU [7] have shown that by placing an electro-optic crystal in contact with the circuit under test, picosecond waveforms could be measured without a hybrid connection. Although these techniques have demonstrated impressive results, they potentially compromise the true device response by reactive loading of the transmission line systems. This occurs due to 1) the fundamental mode mismatch between similar transmission lines on different dielectrics, 2) parasitic reactances associated with the bonding wires between the two transmission line systems or 3) capacitive loading of a transmission line by close proximity to the sampling crystal.

In this paper we report on a new approach to electro-optic sampling of high speed GaAs devices that overcomes these potential limitations. Our system relies on the fact that GaAs is electro-optic and devices and circuits fabricated in this material can be probed directly using picosecond infrared pulses to yield time and frequency domain measurements of a truly noninvasive nature. The circuits can be excited either by on-board photodetectors for impulse response measurements or by external signal generators, phaselocked to the laser pulse train, for analog swept frequency or synchronized digital measurements. In the latter case, the pulse timing stability of the laser becomes an important factor in making accurate measurements. By operating the sampler as a wideband harmonic mixer, we have been able to characterize the timing jitter of the laser and establish the limits it would impose on measurements made with external signal sources.

Of the various possible geometries for electro-optic modulation in GaAs, the longitudinal case illustrated in Fig. 1a is the most attractive. In this configuration, the optical sampling beam passes through the wafer at a point adjacent to the upper conductor of a microstrip transmission line and is reflected back by the ground plane below. For (100) cut GaAs (the most common orientation for integrated circuits), the electric field lines along the (100) axis induce birefringent axes along the (011) and (01$\bar{1}$) directions. This birefringence is converted to an amplitude modulation of the sampling beam with a polarizer. For a given voltage on the transmission line, the electric field (and hence

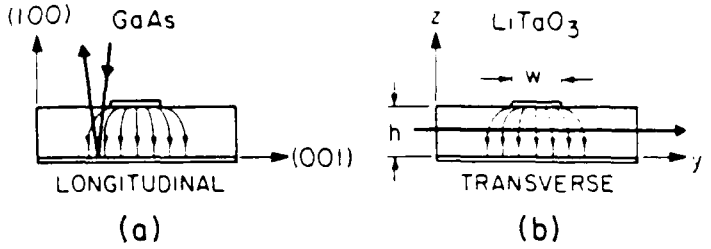

Fig. 1. Microstrip sampling geometries with indicated crystallographic axes.

the birefringence) varies inversely with the substrate thickness. However, since the net phase retardation is proportional to the product of the birefringence and the substrate thickness, the thickness cancels out. The sensitivity, or minimum detectable voltage, is therefore independent of the characteristic impedance of the transmission line and for a 50 Ω microstrip system is nearly ten times better than that of the transverse $LiTaO_3$ sampler (Fig. 1b). Previous approaches to electro-optic sampling relied on a transverse field geometry [1-7] and thus were sensitive to the dimensions of the transmission lines. With this new longitudinal sampling configuration, we can make absolute voltage measurements, independent of transmission line impedances and device geometries.

To make impulse response measurements with on-chip photodetectors, a dual wavelength picosecond source is needed. A Nd:YAG laser is ideal for this application. The 1.06 μm wavelength is well below the absorption edge of GaAs and can be used as the sampling beam. The second harmonic, obtained by frequency doubling to .532 μm, yields an ideally synchronized source for exciting photodetectors. While reliable cw mode-locked Nd:YAG lasers are commercially available, the minimum pulsewidth is limited to 50-100 ps and is too long to be used for high speed sampling. However, recent work on fiber-grating pulse compressors has resulted in the efficient compression of Nd:YAG pulses to less than 5 ps [8]. As a first step toward sampling monolithic GaAs integrated circuits, we used a packaged GaAs photodiode [9] connected to a GaAs microstrip transmission line. We excited the photodiode with 5 picosecond pulses and electro-optically sampled the microstrip line to yield the photodiode impulse response. Although a hybrid arrangement, the initial results demonstrated the effectiveness of the longitudinal sampling geometry. A more complete description of this experiment can be found in [10].

Because an electro-optic modulator produces a photocurrent that is proportional to the product of the optical intensity and the modulating signal, it can be viewed as a mixer. In the frequency domain, any signal at ν_0 propagating on the transmission line will mix with all of the harmonics of the fundamental sampling rate, f_0. Sidebands due to the convolution of these two spectra will appear at frequencies $nf_0 \pm \nu_0$. In particular, if the transmission line is driven with a pure microwave signal, a replica of the nearest harmonic will appear between DC and $f_0/2$, where it can be conveniently viewed on a spectrum analyzer or other receiver. This permits frequency domain measurements to be made throughout the microwave spectrum by driving the circuit under test with an external signal generator and measuring the magnitude of the mixer products at baseband. The phases of the microwave signals are also preserved and any fluctuations or phase noise is transferred to the baseband signal. If the driving signal is a clean sinusoid, the phase noise of the down-converted harmonic is readily apparent and provides a way to quantify the jitter in the laser pulse train. A typical harmonic spectral component

contains a delta function at nf_0 and a phase noise pedestal arising from the pulse-to-pulse timing jitter of the laser. For small phase fluctuations, the relative phase noise power at a given offset from the carrier can be shown to vary as the square of the harmonic number, n [11]. Figure 2 shows a series of harmonic spectra mixed down to about 10 MHz. These spectra were obtained by applying signals up to 16 GHz ($n = 199$) to the transmission line with an HP 8340 microwave synthesizer phase-locked to the laser mode-locker driver (HP 3325). The growth of the phase noise sidebands was found to be in excellent agreement with the predicted square-law dependence.

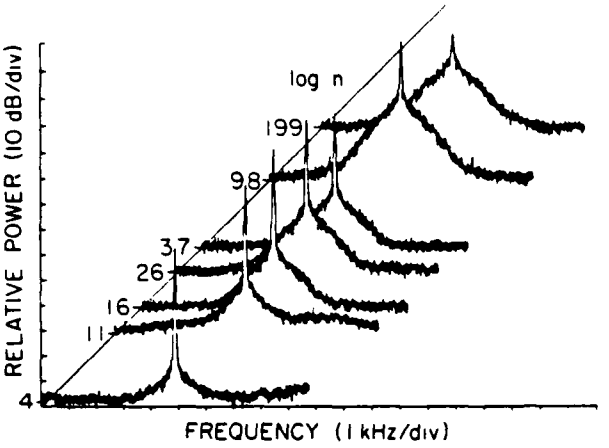

Fig. 2. Laser envelope harmonic spectral components converted to 10 MHz by harmonic mixing in the electro-optic sampler. Center frequency of each component equals $n \times 82$ MHz, where n is the harmonic number.

The power in the phase noise sidebands, P_{DSB}, can be shown to be related to the r.m.s. timing jitter [11,12]. To calculate the total double sideband power, the phase noise spectrum is integrated from some low frequency f_1 near the carrier (nf_0) to some higher frequency f_2 where the phase noise power falls to the level of the AM and Johnson noise. Since the apparent width of the carrier component depends on the resolution bandwidth of the spectrum analyzer, using a narrower bandwidth allows lower frequency phase fluctuations to contribute to the total sideband power. Thus, any calculation of timing jitter using this method must specify the low frequency cutoff, f_1. The expression relating the r.m.s. timing jitter to the carrier power P_c and the phase noise power is

$$\Delta t_{r.m.s.} = \frac{T}{2\pi n}\sqrt{\frac{P_{DSB}}{P_c}} \qquad \text{where} \qquad P_{DSB} = 2\int_{f_1}^{f_2} \frac{P_b(f)}{B}\,df \qquad \text{and } T = 1/f_0$$

Using a spectrum analyzer with a resolution bandwidth of 10 Hz, we determined that $\Delta t_{r.m.s.} \leq 11$ ps for $f_1 \geq 10$ Hz [13]. This suggests that if this pulse train is used to sample a microwave signal and produce less than, say, 10 degrees phase uncertainty, the microwave frequency must be below 2.5 GHz.

In spite of this limitation, we used this pulse train to sample an active monolithic microwave integrated circuit (*mmic*) at a single frequency to observe electronic distortion. We drove a four stage GaAs FET traveling wave amplifier [14] with a microwave synthesizer phase-locked to the laser mode-locker driver. We chose an operating frequency that was an exact multiple of the fundamental sampling rate plus one hertz. Thus, the sampling pulses "walked through" the driving sinusoid at a rate of one hertz. By pulse modulating the synthesizer at 10 MHz, a narrowband receiver could be used for signal-to-noise enhancement. Since the spectrum analyzer we used as the 10

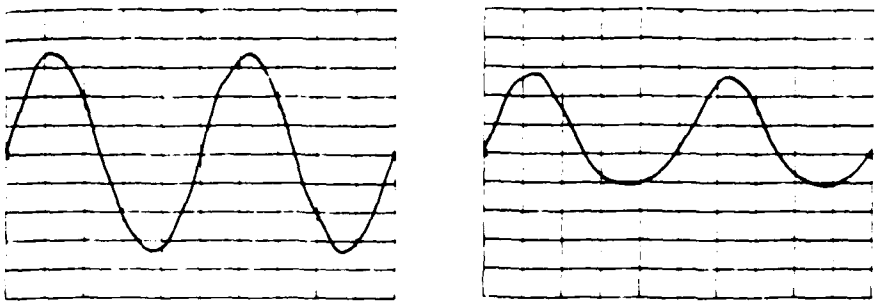

(a) (b)

Fig. 3. Voltage output of a four stage GaAs FET traveling wave amplifier measured by electro-optic sampling in the GaAs substrate. (a) Normal drain-source biasing. (b) Reduced drain-source biasing demonstrating soft clipping distortion. Frequency ≈ 3 GHz. (Horizontal ≈ 65 ps/div. Vertical ≈ .2 volts/div.)

MHz photodiode receiver displayed only the r.m.s. value of the sampled waveform, we injected a small amount of the 10 MHz chopping signal into the input so that it would sum vectorially with the photodiode signal and produce a true bipolar waveform.

With the synthesizer tuned to approximately 3 GHz, and the TWA biased normally, we measured the waveform shown in Fig. 3a by electro-optically sampling the TWA at the output of its last stage. Then, we reduced the drain-to-source voltage (V_{DS}) from +4 volts to +1.5 volts so that the TWA was operating in the "triode region". Figure 3b shows the soft clipping on the negative peaks as well as the reduction in gain that resulted from this bias condition.

Acknowledgements

The authors wish to thank George Zdasiuk of Varian Associates for supplying the GaAs FET TWA. They also wish to acknowledge the partial support of the Air Force Office of Scientific Research and the Joint Services Electronics Program.

References

1. J.A. Valdmanis, G. Mourou, and C.W. Gabel: *Appl. Phys. Lett.*, **41**, 211 (1982)
2. J.A. Valdmanis, G. Mourou, and C.W. Gabel: *IEEE J. Quant. Elect.*, **19**, 664 (1983)
3. G.A. Mourou and K.E. Meyer: *Appl. Phys. Lett.*, **45**, 492 (1984)
4. B.H. Kolner, D.M. Bloom, and P.S. Cross: *Elect. Lett.*, **19**, 574 (1983)
5. B.H. Kolner, D.M. Bloom, and P.S. Cross: *SPIE Proceedings*, **439**, 149 (1983)
6. J.A. Valdmanis, G. Mourou, and C.W. Gabel: *SPIE Proceedings*, **439**, 142 (1983)
7. K.E. Meyer and G.A. Mourou: unpublished
8. J.D. Kafka, B.H. Kolner, T.M. Baer, and D.M. Bloom: *Optics Lett.*, **9**, 505 (1984)
9. S.Y. Wang, D.M. Bloom, and D.M. Collins: *Appl. Phys. Lett.*, **42**, 190 (1983)
10. B.H. Kolner and D.M. Bloom: *Elect. Lett.*, **20**, 818 (1984)
11. J. Kluge: *Ph.D. Thesis*, Universistät Essen, Fed. Rep. of Germany (1984)
12. W.P. Robins: "Phase Noise in Signal Sources", Peter Peregrinus Ltd., London (1982)
13. B.H. Kolner, K.J. Weingarten, and D.M. Bloom: *SPIE Proc.*, **539**, (1985) to be published
14. Laboratory prototype, courtesy of Varian Associates

DIRECT ELECTRO-OPTIC SAMPLING OF GaAs INTEGRATED CIRCUITS

Indexing terms: Integrated circuits, Electro-optics

We report the first electro-optic sampling measurements made directly within an integrated circuit. Using the electro-optic effect in GaAs, we have noninvasively probed the internal voltage waveforms of a 2–12 GHz GaAs FET travelling-wave amplifier integrated circuit driven by a microwave signal source.

To characterise GaAs monolithic microwave integrated circuits (MMICs) and very-high-speed digital integrated circuits fully demands noninvasive measurements of the internal voltage waveforms of the circuits at frequencies exceeding 50 GHz. Conventional sampling oscilloscopes and network analysers have limited bandwidths and cannot probe points internal to an IC without seriously degrading device performance.

Electro-optic sampling of high-speed electronics is motivated by the ability of laser systems to produce ultrashort light pulses and then, through the electro-optic effect, sense electrical waveforms. Within an electro-optic crystal, the electric fields associated with circuit voltages induce birefringence, causing a polarisation change to incident light. When the polarisation-modulated light is passed through an analysing polariser, the resulting amplitude modulation is proportional to the electric field.

Previous sampling experiments[1,2] have used a hybrid

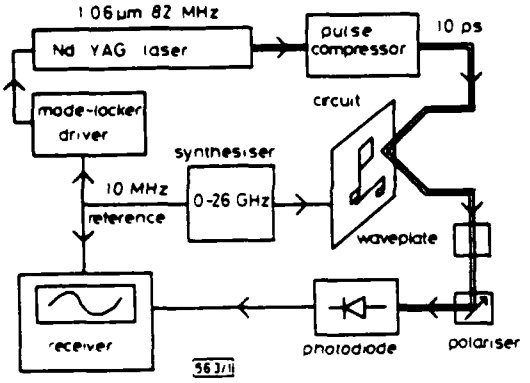

Fig. 1 *Electro-optic sampling system*

approach, with the terminals of the electrical device under test connected to a transmission line deposited on an electro-optic crystal. While this approach has demonstrated very wide bandwidth capabilities, the parasitic reactances associated with the device-crystal interconnection will significantly degrade device performance at high frequencies. In addition, points internal to an integrated circuit cannot be probed.

GaAs is itself electro-optic, and hence sampling can be performed directly in the substrate of a GaAs IC. Kolner and Bloom have used a longitudinal geometry to sample the fringing electric fields of a microstrip transmission line deposited on (100)-cut GaAs.[3] We report here the application of this geometry to the measurement of microwave signals within a GaAs FET travelling-wave amplifier (TWA). Because no external electro-optic crystal is connected to the circuit, device performance is undisturbed and arbitrary points within the circuit can be probed.

Initial demonstrations of electro-optic sampling[1] and of direct electro-optic sampling in GaAs[3] used a pump-probe technique, where the measured impulse response was excited by fast photodevices, triggered from a portion of the same light beam that provided the sampling pulses. For many circuits sinewaves or squarewaves from an external signal generator are more appropriate test signals than are impulses from a photodetector. If the external signal source is tuned to an exact harmonic N of f, where f is the pulse repetition rate of a mode-locked laser, N is the harmonic number, the same point in the circuit is sampled every N cycles. The phase of the external generator can then be varied with respect to the laser pulse train to map out the waveform.

The sampling system (Fig. 1) consists of a mode-locked Nd:YAG laser producing 1·06 μm, 100 ps pulses at an 82 MHz rate. A fibre-grating pulse compressor shortens the pulses to 10 ps, increasing the sampler bandwidth.[4] The beam is focused to 10 μm diameter next to a transmission line on the TWA. The light is reflected off the metallised back of the substrate, collected and recollimated with the focusing lens, and directed through an analysing polariser on to a photodiode. The microwave excitation to the TWA is pulse-modulated to translate the measurement from DC to 10 MHz, above the low-frequency amplitude noise of the laser. A spec-

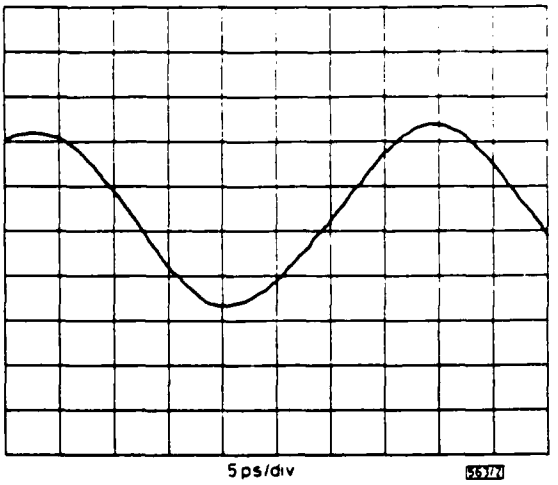

Fig. 2 *26·4 GHz waveform on gate line of travelling-wave amplifier*

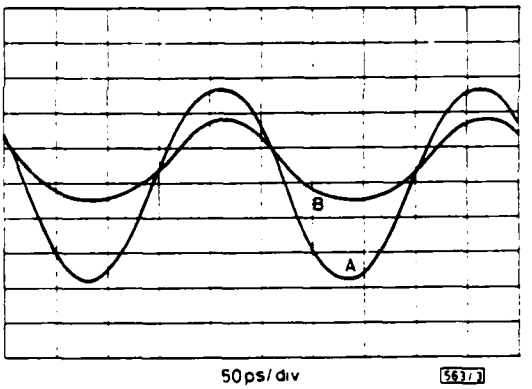

Fig. 3 *4 GHz waveforms on drain line of travelling-wave amplifier measured by electro-optic sampling*

Trace A: Normal drain bias
Trace B: Reduced drain bias causing soft clipping

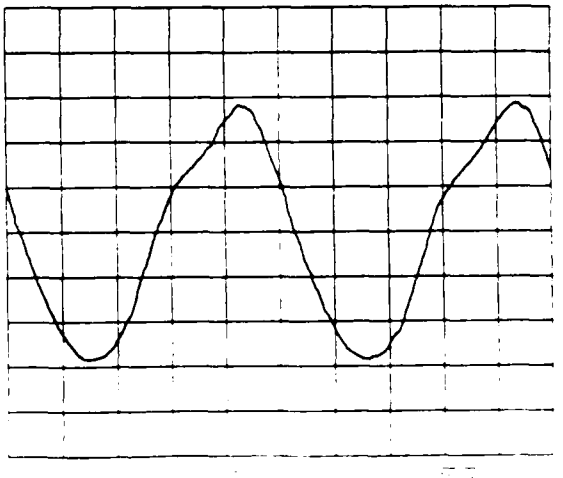

Fig. 4 *Input signal a[illegible] forward[illegible] Hz*

Reprinted from ELECTRONICS LETTERS 15th August 1985 Vol. 21 No. 17 pp. 765-766

trum analyser acts as a fixed-frequency receiver to display the waveform. Since the spectrum analyser measures only signal magnitude, we inject a reference 10 MHz carrier in phase with the receiver photocurrent to reconstruct a bipolar waveform.

When an external signal source is used the phase stability of the laser with respect to this source becomes important. The phase noise of many commercial microwave synthesisers corresponds to timing jitter of less than 1 ps. However, initial phase-noise measurements[5] indicate timing jitter in the order of 10 ps RMS arising from the laser system. To combat this noise a phase-locked loop was implemented around the laser, reducing jitter to 1·5 ps RMS and providing a phase reference for relative phase measurements and signal averaging.

The temporal resolution of this sampler system currently is limited by the optical pulsewidth of 10 ps. Other resolution limits include the electrical transit time (ETT) of the signal moving past the spatial extent of the optical beam, the optical transit time (OTT) of the beam as it passes twice through the substrate and the pulse-to-pulse timing jitter of the laser. The ETT for a 10 μm-diameter beam is $\simeq$0·1 ps and the OTT for the 100 μm substrate thickness of the 12 GHz TWA used in these experiments is 2·4 ps. Higher-frequency devices typically have thinner substrates and the OTT decreases. The fibre-grating compressor has demonstrated compression of mode-locked Nd:YAG to less than 1 ps,[6] and recent work in this laboratory indicates the jitter of the laser can also be further reduced to less than 1 ps. Such improvements would result in a system bandwidth of roughly 400 GHz.

Fig. 2 shows a signal measured on the gate line of the TWA.† Although the device bandwidth is 12 GHz, signals to 26 GHz, the limit of our microwave source, were measured. Since the sampler bandwidth is large enough to include harmonics of signals in the device's operating range, waveforms with distortion can be detected. Fig. 3 shows distortion deliberately introduced by varying the device's DC bias. By lowering the drain-source bias voltage the gain is reduced and clipping is observed on one side of the waveform. Overdriving the input to the device causes forward gate conduction as evidenced by the waveform of Fig. 4.

In conclusion, the electro-optic sampler provides a technique for noncontact, noninvasive signal measurements for high-frequency circuits and devices. Since 1·06 μm optical pulses as short as 1 ps, and laser timing jitter as small as 1·5 ps have been demonstrated, the potential bandwidth of the system is several hundred gigahertz. This sampling technique is adaptable to many high-frequency measurements, is not limited to the transmission-line reflection geometry, and has application to both analogue and digital circuits. Since vector measurements are possible, this technique forms the basis for noninvasive wideband network analysis.

† Laboratory prototype, courtesy of Varian Associates

Acknowledgments: The authors wish to thank G. Zdasiuk of Varian Associates for supplying the GaAs FET TWA and for his invaluable assistance. This work was supported by the Air Force Office of Scientific Research and the Joint Services Electronics Program.

K. J. WEINGARTEN
M. J. W. RODWELL
H. K. HEINRICH
B. H. KOLNER
D. M. BLOOM

Edward L. Ginzton Laboratory
Stanford University
Stanford, CA 94305, USA

15th July 1985

References

1 VALDMANIS, J. A., MOUROU, G., and GABEL, C. W.: 'Picosecond electro-optic sampling system', *Appl. Phys., Lett.*, 1982, **41**, pp. 211–212

2 KOLNER, B. H., BLOOM, D. B., and CROSS, P. S.: 'Electro-optic sampling with picosecond resolution', *Electron. Lett.*, 1983, **19**, pp. 574–575

3 KOLNER, B. H., and BLOOM, D. B.: 'Direct electro-optic sampling of transmission-line signals propagating on a GaAs substrate', *ibid.*, 1984, **20**, pp. 818–819

4 KAFKA, J. D., KOLNER, B. H., BAER, T., and BLOOM, D. M.: 'Compression of pulses from a continuous-wave mode-locked Nd:YAG laser', *Opt. Lett.*, 1984, **9**, pp. 505–506

5 KOLNER, B. H., WEINGARTEN, K. J., and BLOOM, D. B.: 'Electro-optic sampler for gallium arsenide integrated circuits', Proceedings of SPIE on ultrashort pulse spectroscopy and applications, 1985, **533**, pp. 139–143

6 HERITAGE, J. A., WEINER, A. M., and THURSTON, R. N.: 'Picosecond pulse shape manipulation'. Technical digest of conference on lasers and electro-optics, Baltimore, Maryland, 1985, pp. 98–100

Electro-optic sampling of planar digital GaAs integrated circuits

J. L. Freeman, S. K. Diamond, H. Fong, and D. M. Bloom
Stanford University, Edward L. Ginzton Laboratory, Stanford, California 94305

(Received 22 July 1985; accepted for publication 27 August 1985)

We report a new electro-optic sampling configuration which allows planar digital GaAs circuits to be probed noninvasively. Our technique employs a novel backside reflecting geometry, in which a laser beam enters the GaAs substrate from the back and reflects from the circuit metallization. By combining the electro-optic effect in GaAs with sub-band-gap (1.06 μm) picosecond pulses from a continuous wave, mode-locked neodymium:yttrium aluminum garnet laser, we are able to make wide-band voltage measurements within GaAs integrated circuits. Results are presented of signals measured on the 2-μm-wide on-chip output line of a medium scale integrated multiplexer/demultiplexer clocked at 2.6 GHz.

With increasing numbers of medium and large scale integrated logic circuits that operate at gigahertz frequencies, an urgent need has arisen for measurements of digital waveforms at various points in such circuits. Conventional sampling oscilloscopes and probe stations have limited bandwidths and cannot probe on-chip waveforms noninvasively. Previous electro-optic sampling systems have used microstrip and coplanar transmission line structures in $LiTaO_3$[1,2] as well as GaAs monolithic microwave integrated circuits (MMIC).[3,4] In this letter, we describe a new approach to electro-optic sampling of GaAs circuits which permits noninvasive, wide-band measurements of voltage levels, independent of specific conductor geometries, and its recent application to a high-speed planar medium scale integration (MSI) logic circuit.

In a GaAs crystal the electric field of an applied signal induces optical birefringence specified by an ellipse obtained from the intersection of the plane normal to the direction of propagation with the index ellipsoid for the given local field configuration.[5] For GaAs, a crystal of the zincblende ($\bar{4}3m$) structure, the ellipsoid takes the form

$$(x^2 + y^2 + z^2)/n_0^2 + 2r_{41}(E_x\, yz + E_y\, xz + E_z x\, y) = 1, \tag{1}$$

where x, y, and z are along the [100], [010], and [001] axes respectively, r_{41} is the nonzero element of the electro-optic tensor for $\bar{4}3m$ crystals, and n_0 is the index of refraction for GaAs.[6] In GaAs device fabrication, the most commonly used substrate orientation is (100).[7] Hence, in our geometry, shown in Fig. 1, light will be incident along [100] and will produce an index ellipse described by

$$(y^2 + z^2)/n_0^2 + 2r_{41}E_x\, yz = 1, \tag{2}$$

which has axes y' and z' at 45° with respect to y and z and values

$$n_{y'} \doteq n_0 + \tfrac{1}{2} n_0^3 r_{41} E_x,$$
$$n_{z'} \doteq n_0 - \tfrac{1}{2} n_0^3 r_{41} E_x. \tag{3}$$

Note that in this geometry, only the longitudinal field component modulates the beam optical properties.

As the optical beam propagates through the crystal (see Fig. 1), the birefringence in (3) introduces a change in phase between the y' and z' components of the light proportional to $\int E_x\, dx$. This, however, may be recognized as simply the voltage difference between the two limits of integration—the metal line and the substrate backside—since voltage is just the path-independent line integral of the electric field from one point to another. In high-speed logic circuits, where the thickness of the crystal substrate is typically much greater than the separation between metal lines on the surface, the backside is essentially at zero potential and $\int E_x\, dx = V_{sig}(t)$. The minimum detectable voltage for this geometry is the same as that for the microstrip geometry which for typical photodiode currents is 22 $\mu V/\sqrt{Hz}$.[3]

Several advantages of this novel approach are evident when compared with previous electro-optic sampling techniques: first, any conductor geometry can be probed since the measured value is $V_{sig}(t)$ for any field configuration; second, very small, closely spaced points may be examined, limited only by the spot size of the beam, since the potential measured is that on the conductor, and is not influenced by the potential on adjacent lines. Both these features are essential to the accurate testing of medium and large scale integration circuits.

The key components of the measurement system are shown in Fig. 2. Mode-locked 1.06 μm light pulses of approximately 10 ps duration and repetition rate $f_0 = 82$ MHz are generated from a commercially available neodymium: yttrium aluminum garnet laser in conjunction with a fiber-grating pulse compressor.[8] The light beam is passed through a polarizing beamsplitter cube and focused by a microscope objective through a small hole in the integrated circuit carrier to a 3 μm spot at the GaAs surface. After reflection from

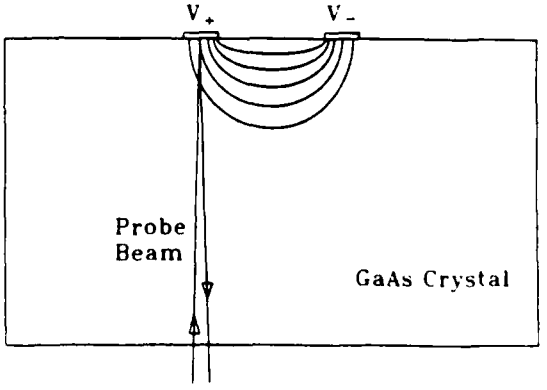

FIG. 1. New sampling geometry for electro-optically probing planar digital GaAs integrated circuits.

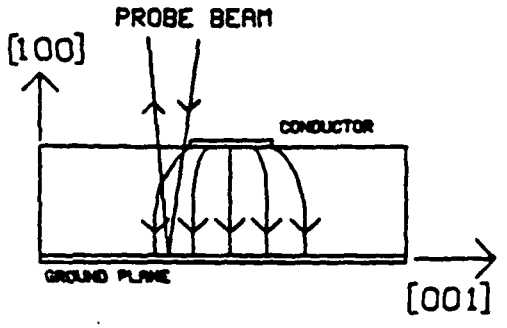

Figure 2: Frontside reflection geometry for probing GaAs MMIC's.

SAMPLING OF INTEGRATED CIRCUITS

Initial demonstrations of electro-optic sampling (1) and of direct electro-optic sampling in GaAs (3) used a pump-probe technique. A pulsed laser system produces short pulses of light to trigger fast photodiodes or photoconductors to generate electrical waveforms. Pulses from the same laser then electro-optically sample the electrical response, and by varying the relative delay time between the trigger and the probe beams to the circuit, the electrical waveform is mapped in time. For many circuits, however, sinewaves or squarewaves from an external signal generator are more appropriate test signals than are impulses from a photodetector. If the external signal source is tuned to an exact harmonic nf_0 of the laser pulse repetition rate f_0, the same point on the circuit waveform is sampled every nth cycle. The phase of the signal generator is then varied with respect to the laser pulse train to map out the waveform. In these experiments, the microwave signal is offset a few herts from nf_0, providing a continuous phase shift to display the waveforms in real-time.

A cw mode-locked Nd:YAG laser provides 1.06 μm light pulses of 100 ps duration at a repetition rate $f_0 = 82$ MHz which are shortened to 5 ps with a fiber-grating pulse compressor (5). After interacting with the device under test, the phase-modulated beam is directed to an analysing polarizer and onto a photodiode to detect the amplitude modulation. For these experiments, the signal of interest is modulated (typically at 10 MHz) to bring the signal above the low-frequency amplitude noise of the laser, and a spectrum analyser acts as a fixed frequency receiver.

When an external signal source is used, the phase stability of the laser with respect to this source becomes important. The phase noise of many commercial microwave synthesizers corresponds to timing jitter of less than 1 ps. However, initial phase noise measurements (6) indicate timing jitter on the order of 10 ps rms arising from the laser system, even when driven with a very stable RF signal.

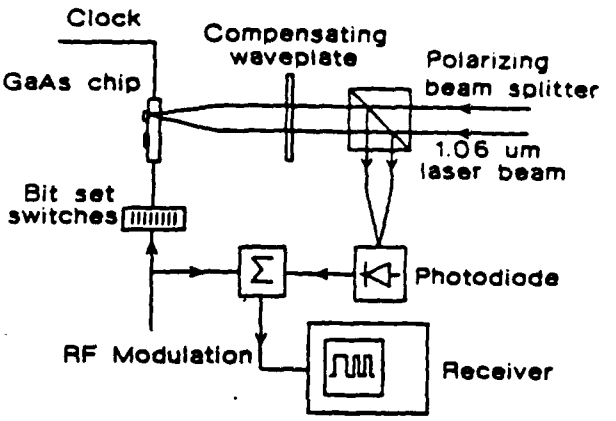

Figure 3: Experimental setup for probing digital GaAs integrated circuits.

To combat this noise a phase-lock-loop was implemented around the laser, reducing the jitter to 2 ps rms. Long term timing drift is typically a few picoseconds per minute, providing good timing stability for relative phase measurements and signal averaging.

The temporal resolution of this sampler system is currently limited by the optical pulse width of 5 ps. Other resolution limits include the electrical transit time (ETT) of the signal moving past the spatial extent of the optical beam, the optical transit time (OTT) of the beam as it passes twice through the substrate, and the pulse-to-pulse timing jitter of the laser. The ETT for a 10 μm diameter beam is $\approx$ 0.1 ps and the OTT for the 100 μm substrate thickness of the 12 GHz TWA used in these experiments is 2.4 ps. Higher frequency devices typically have thinner substrates and the OTT decreases. The fiber-grating compressor has demonstrated compression of mode-locked Nd:YAG to less then 1 ps (7), and recent work in this lab indicates the jitter of the laser can also be further reduced to less than 1 ps. Such improvements would result in a system bandwidth of roughly 400 GHz.

High Speed Planar Digital Circuits

The key components of the system used for probing of digital circuits (8) are shown in Figure 3. The light beam is passed through a polarising beamsplitter cube and focused by a microscope objective through a small hole in the IC carrier to a 2.9μm spot (FWHM) at the GaAs surface. After reflection from the conductor, the beam is recollimated by the objective, and the returning beam is deflected by the polarizing beamsplitter to a photodetector. A compensating waveplate biases the round-trip polarization shift to $\lambda/4$ for maximum sensitivity at the receiver photodiode.

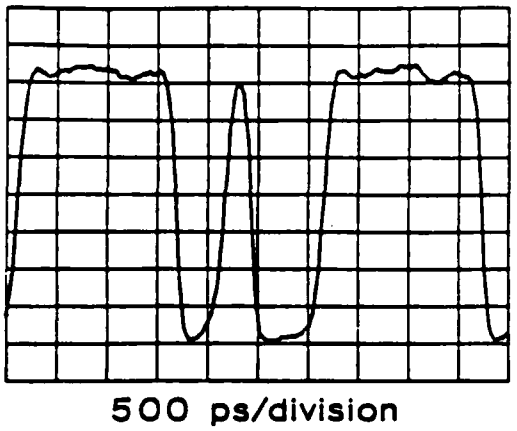

Figure 4: Electro-optically sampled serial output waveform of a 2.6 gigahertz multiplexer/demultiplexer just before the output buffer amplifier. The parallel input word is 11110100 (b0...b7).

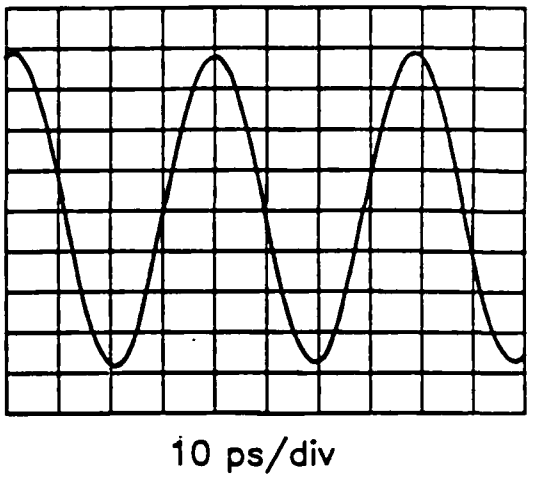

Figure 6: 26 GHz waveform on gate line of TWA.

We have applied this system to the measurement of voltage waveforms within an 8-bit multiplexer/demultiplexer (9) clocked at 2.6 GHz. The eight parallel input lines were set by a bank of switches, and the serial output signal of the multiplexer on a 2μm wide line leading to the output buffer stage was probed. In Figure 4 we show the electro-optically sampled serial waveform that corresponds to the parallel input word 11110100 (b0...b7). The relative position of each bit could be confirmed by changing the setting of the bit switches and observing the change of the waveform in real-time.

Monolithic Microwave Integrated Circuits

The MMIC sampling system (10) is shown in Figure 5. The beam is focused to 10 microns diameter next to a transmission line on the travelling wave amplifier (TWA) (11). The light is reflected off the metallized back of the substrate, collected and recollimated with the focusing lens, and directed through an analysing polarizer onto a photodiode. The microwave excitation to the TWA is pulse modulated at 10 MHz for detection by a spectrum analyzer to display the time waveform.

Figure 6 shows a signal measured on the gate line of the TWA (11). Although the device bandwidth is 12 GHz, signals to 26 GHz, the limit of our microwave source, were measured. Since the sampler bandwidth is large enough to include harmonics of signal in the device's operating range, waveforms with distortion can be detected. Figure 7 shows distortion along the drain (output) line deliberately introduced by overdriving the input.

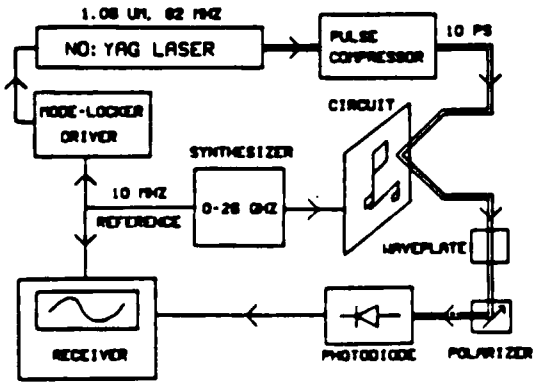

Figure 5: Experimental setup for MMIC measurements.

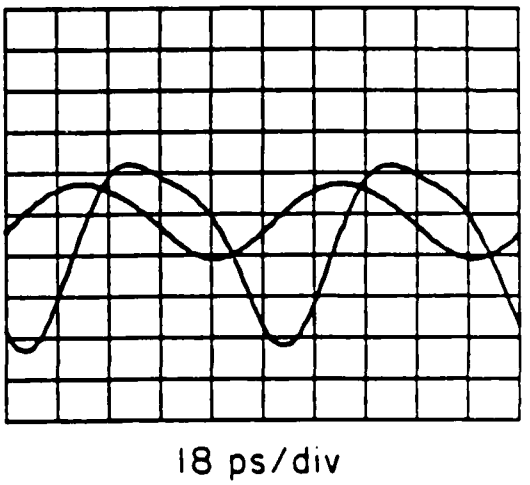

Figure 7: 11 GHz waveforms on drain line of traveling wave amplifier measured by electro-optic sampling. Normal waveform at 0 dBm input power, distorted waveform at 15 dBm. Voltage scale inverted.

CHARACTERIZATION OF GaAs INTEGRATED CIRCUITS BY DIRECT ELECTRO-OPTIC SAMPLING

K.J. Weingarten, M.J.W. Rodwell, J.L. Freeman, S.K. Diamond and D.M. Bloom

Edward L. Ginzton Laboratory, Stanford University
Stanford, California 94305

ABSTRACT

With the recent demonstration of direct electro-optic sampling of GaAs circuits, a new method to characterize high-speed monolithic microwave and digital circuits exists. This technique uses picosecond pulses from a laser to non-invasively probe voltage waveforms at points internal to monolithic circuits with a measurement bandwidth in excess of 50 GHz. This paper presents measurements of a GaAs MESFET traveling wave amplifier and an 8-bit multiplexer/demultiplexer.

INTRODUCTION

Recent monolithic microwave integrated circuits (MMIC's) and high-speed logic circuits (1-2) exceed the characterization capabilities of conventional test instruments. Sampling oscilloscopes have rise times of 25 picoseconds (ps) while network analyzers, with added external source multipliers and mixers and complex error correction make vector measurements to about 100 GHz. Neither system can probe points internal to a circuit without serious loading effects.

Ultrashort pulse laser systems, however, can generate light pulses of less than 10 femtoseconds duration (3). The electro-optic effect provides a way to use such short optical pulses to measure electrical waveforms (4-5). The electro-optic effect in GaAs has a response time of about a femtosecond.

ELECTRO-OPTIC SAMPLING DIRECTLY IN GaAs

Since gallium arsenide is electro-optic an applied electrical field will induce a small optical birefringence in the GaAs crystal. Incident light senses this birefringence by a change in its polarization. A polarizer converts the change in polarization to a change in intensity. Due to the nature of the electro-optic tensor in GaAs and the longitudinal probe beam geometry used (Fig. 1, Fig. 2), this change in intensity is proportional to the voltage across the GaAs substrate (6-8).

To achieve short temporal resolution, a cw mode-locked Nd:YAG/fiber-grating pulse compressor system (9) producing 5 ps pulses of 1.06 μm light is used as the probe beam. Since the photon

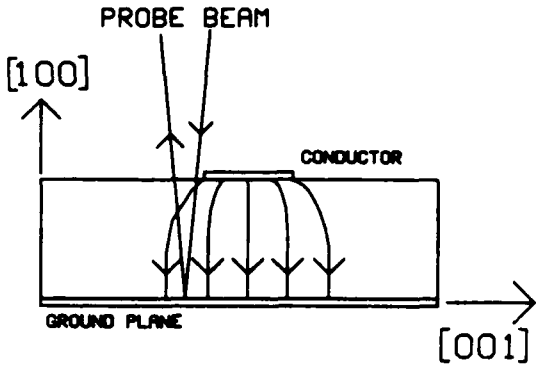

Figure 1. Front-side reflection geometry suitable for probing MMIC transmission line. Typical conductor width is less than 40 μm and typical substrate thickness is 100 μm.

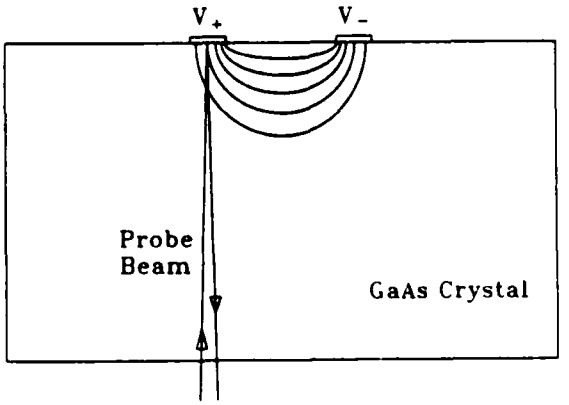

Figure 2. Back-side reflection geometry suitable for digital or analog circuits with lumped-element interconnects. Typical conductor width is less than 5 μm while substrate thickness is several hundred microns.

CH2252-5/85/0000/0479 $1.00 © 1985 IEEE

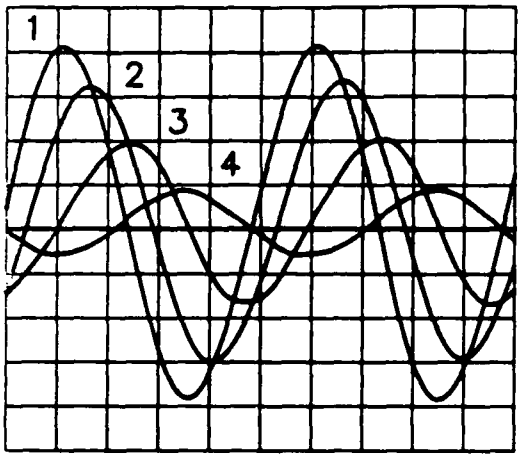

Figure 5. Waveforms at the gate of each FET, numbered from input (1) to output (4). Operating frequency is 8.2 GHz, input power is 0 dBm.

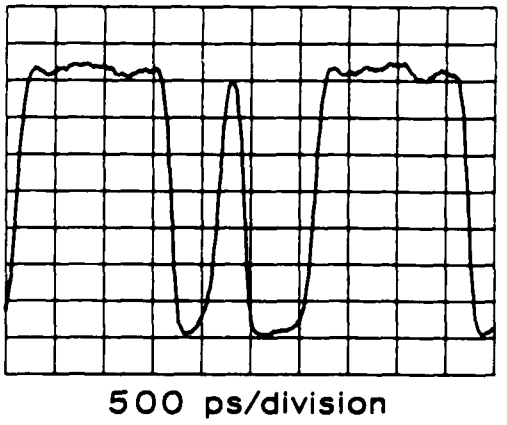

Figure 7. Serial output word measured internal to the circuit's output buffer. The clock rate is 2.6 GHz and the multiplexed word is 11110100.

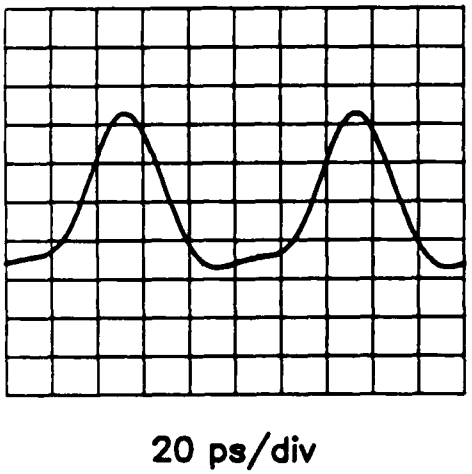

Figure 6. Distortion at the second FET drain at 15 dBm input power.

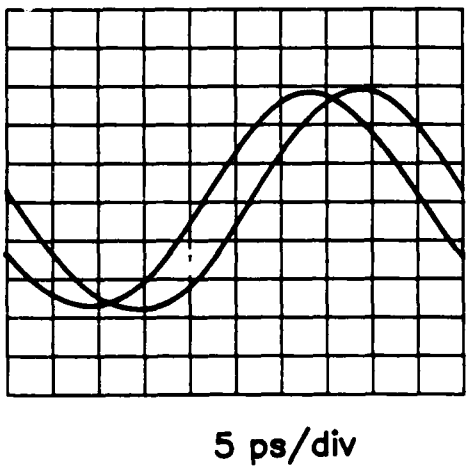

Figure 8. 20 GHz signals measured at the input of the TWA. The 5 ps optical delay is generated with a stepper motor.

The circuit used in this experiment was a medium-scale integration 8-bit multiplexer/demultiplexer (MUX/DEMUX) implemented in GaAs buffered-FET logic (13). Figure 7 shows a typical waveform measured on the serial output line of the MUX prior to the output buffer stage.

Electrooptic Sampling in GaAs Integrated Circuits

BRIAN H. KOLNER, STUDENT MEMBER, AND DAVID M. BLOOM, MEMBER, IEEE

(Invited Paper)

Abstract—**Electrooptic sampling has been shown to be a very powerful technique for making time-domain measurements of fast electronic devices and circuits. Previous embodiments relied on a hybrid connection between the device under test and a transmission line deposited on an electrooptic substrate such as $LiTaO_3$. The hybrid nature of this approach leads to device packaging difficulties and can result in measurement inaccuracies and performance degradation at very high frequencies. Since GaAs is electrooptic and an attractive material for high speed devices, we have devised an approach of direct electrooptic sampling of voltage waveforms in the host semiconductor. In this paper, we review the principles and limitations of electrooptic sampling and discuss this new noninvasive technique for electronic probing with applications to characterizing high speed GaAs circuits and devices.**

I. Introduction

THE speed of solid-state electronic and optoelectronic devices has steadily increased over the years, continually challenging our ability to measure them. Indeed, the improvements in instrumentation have often been driven by these constant advances in device performance. Sampling oscilloscopes can resolve risetimes approaching 25 ps, but state-of-the-art transistors employing novel structures have already broken the 10 ps barrier [1] and photoconductive switches have been demonstrated with subpicosecond response times [2].

On the other hand, techniques for ultrashort optical pulse generation and measurement have improved at an even faster rate and, today, light pulses as short as 8 fs have been generated [3]. The question of how to utilize these ultrashort light pulses to make electrical measurements has been addressed by several workers over the years using a variety of methods [4]–[7]. Recently, a new electrooptic sampling technique, first reported by Valdmanis *et al.*, was used to repetitively sample the electric field below a transmission line excited by a photoconductive switch [8]. Later, Kolner *et al.* demonstrated a similar system which was used to characterize the performance of a 100 GHz bandwidth GaAs Schottky photodiode [9].

We have recently employed this electrooptic sampling technique to directly probe electrical waveforms propagating on a GaAs substrate containing active devices and transmission line structures [10], [11]. Our approach eliminates the need for hybrid connections between the device under test and an external electrooptic crystal thus allowing noncontact, noninvasive optical probing of GaAs circuits with picosecond time resolution.

In this paper, we review the basic principles of electrooptic sampling and the factors that influence the ultimate time resolution and voltage sensitivity. Second, we discuss methods of noninvasive probing of microwave and digital GaAs integrated circuits by using phase-lock techniques to synchronize a mode-locked laser to a microwave synthesizer and electrooptically sample a circuit in a manner analogous to a sampling oscilloscope. Finally, we present the results of measurements made on a GaAs monolithic microwave integrated circuit (MMIC) that demonstrates the power and flexibility of this new technique.

II. Approaches to Noninvasive Electrical Measurements

Most previous electrooptic sampling systems relied on a hybrid connection between the device under test and a transmission line formed on an electrooptic substrate such as $LiTaO_3$ [8], [9], [12]–[14]. The electric field of the transmission line was then probed transversely [Fig. 1(a)] with ultrashort optical pulses from a mode-locked laser. Although these systems demonstrated outstanding speed and sensitivity, their hybrid nature represents a compromise when very wide bandwidth measurements are anticipated. The physical connection between the device under test and an $LiTaO_3$ transmission line will, for example, introduce parasitic capacitances and inductances that could seriously affect the accuracy of the measurement. One approach that attempted to minimize the effects of this transition was to form a coplanar transmission line at the active device and continue the line to the edge of the substrate where a coplanar transmission line on $LiTaO_3$ with exactly the same dimensions was joined [15]. In this case, the active device was a photoconductive switch formed on a Cr-doped GaAs substrate. Although the physical dimensions of the coplanar lines were exactly matched, the large discontinuity in dielectric constants ($\epsilon_r(GaAs) = 12.3$, $\epsilon_r(LiTaO_3) = 43$), implies that a mode mismatch and reactive energy storage effects occur at the boundary [16].

Another approach to electrooptic sampling in $LiTaO_3$ relied on placing the electrooptic crystal in contact with (or close proximity to) the transmission line to be sampled [14], [17]. The sampling beam was passed through the crystal where fringing fields from the transmission line produced the phase retardation. Using this method, a sampling crystal can be positioned anywhere on a circuit where a measurement is to be made, thereby avoiding a hard-

Manuscript received July 16, 1985; revised September 19, 1985. This work was supported in part by the Air Force Office of Scientific Research and the Joint Services Electronics Program.

B. N. Kolner was with the Edward L. Ginzton Laboratory, Stanford University, Stanford, CA 94305. He is now with Hewlett-Packard Laboratories, Palo Alto, CA 94304.

D. M. Bloom is with the Edward L. Ginzton Laboratory, Stanford University, Stanford, CA 94305.

IEEE Log Number 8406315.

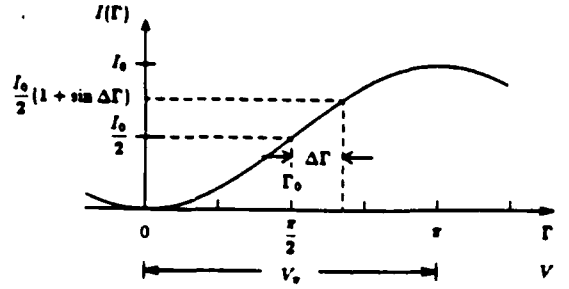

Fig. 2. Light intensity versus net phase retardation Γ or applied voltage V for a Pockels cell light modulator. Static retardation Γ_0 shown at quarter-wave bias point with signal term $\Delta\Gamma$ as a perturbation.

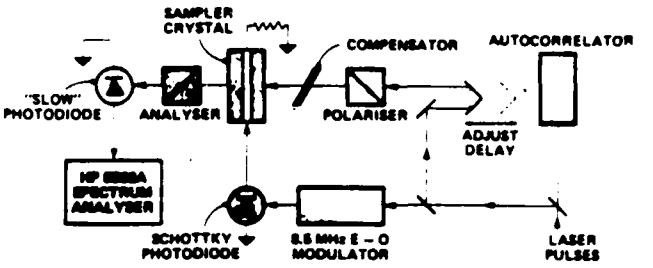

Fig. 3. Schematic diagram of the electrooptic sampling system used to characterize high speed GaAs photodiodes.

mitted light intensity to the applied voltage and is given by

$$I = I_0 \sin^2\left(\frac{\Gamma_0 + \Delta\Gamma}{2}\right) \tag{1}$$

where Γ_0 is the static phase retardation and $\Delta\Gamma$ is the additional retardation induced by the applied electric field (Fig. 2). The static phase retardation plays an important role as the operating point or "bias point." In order to maintain the most linear relationship between the applied voltage and the transmitted light intensity, the modulator must be biased such that $\Gamma_0 = \pi/2$. This point is usually referred to as the *quarter-wave* bias point because it corresponds to a net quarter wave of phase shift between the two polarization components of the optical beam. The voltage required to switch the modulator from the "off" to the "on" state is similarly known as the *half-wave* switching voltage (V_π) and corresponds to a total retardation of π radians. Thus, at the quarter-wave bias point, we can write (1) as

$$I = \frac{I_0}{2}(1 + \sin \Delta\Gamma) = \frac{I_0}{2}\left(1 + \sin \pi \frac{V}{V_\pi}\right) \tag{2}$$

The basic components of an electrooptic sampling system are illustrated in Fig. 3. In this arrangement, the impulse response of a high speed GaAs Schottky photodiode is to be measured. The photodiode has been connected to a microstrip transmission line deposited on an electrooptic crystal which, together with a polarizer and orthogonally oriented analyzer, constitutes the Pockels cell light modulator. A train of picosecond optical pulses from a mode-locked laser is split into three beams with the first beam incident on a scanning autocorrelator used for laser diagnostics. The second, lower beam is used to illuminate the photodiode under test which injects a current pulse onto the transmission line with each optical pulse. If the duration of the optical pulse is short compared to the impulse response of the photodiode, then the propagating electric field represents the photodiode impulse response. A high frequency electrooptic modulator has been included in the excitation path to put modulation sidebands on the photocurrent so that a narrow-band receiver can be used to improve the signal-to-noise ratio (Section IV). The remaining pulses in the upper beam are routed through a delay leg so that when they arrive at the transmission line, they will exactly coincide with the photocurrent waveform produced by a replica of that same pulse. As each pulse passes through the electric field beneath the line, it interacts with a small portion of the photocurrent waveform and experiences a modulation proportional to the amplitude of the field there. For a fixed path delay between the two beams, the pulses "sample" only one portion of the waveform and thus the average power in the sampling beam is constant. Now, if the delay is adjusted so that the sampling beam path is slightly longer, then the sampling pulses will arrive at the transmission line a little later and interact with a later portion of the photocurrent waveform. As a result, the average power in the sampling beam will be different, representative of the magnitude of the photocurrent at that later point in time. By adjusting the relative path lengths between the excitation and sampling beams, the equivalent impulse response of the high speed photodiode is mapped out in terms of the average sampling beam power exiting the Pockels cell.

Adjustment of the relative path delay can be accomplished in several ways. The most common method is to mount a cube-corner reflector on a mechanically driven stage and route either beam through it. An alternative approach is to use a spinning prism assembly in which the beams are refracted through varying path lengths. This, however, requires a greater length of glass, producing dispersion as well as linearity problems. Another solution is to use two picosecond light sources running at slightly different pulse rates. The sampling pulses constantly "walk" through the excitation pulses and no moving parts are required. Regardless of the approach, the rate at which the measured waveform is acquired determines the bandwidth presented at the sampler output. As we will see, most of the system noise contributions have uniform power spectral densities, thus narrower bandwidths and slower scan rates give higher signal-to-noise ratios.

Fig. 4 shows a detailed view of the interaction between the propagating microwave field $E_z(x, y, z, t)$ and the optical sampling pulse $I(x, y, z, t)$. In this diagram, a microstrip transmission line supports a $+y$-propagating electric field interacting with a $+x$-propagating sampling pulse. A variable time delay τ is included in the arrival time of the sampling pulse. The output signal intensity $I_{sig}(t, \tau)$ represents the sampling pulse profile after being affected by the field-induced phase retardation. When there is no overlap between the fields, $I_{sig}(t, \tau) = 0$. Since the slow photodiode measuring the sampling beam power can-

where nL/c is the optical transit time through the transmission line electric field.

B. Electrical Transit Time Effect

The OTT accounted for the degradation of the impulse response due to the sampling beam propagating across the width of the transmission line and the resultant impulse response was calculated by assuming that all fields had inifinitesimal spatial and temporal extent except for the width of the transmission line field. The *electrical transit time effect* (ETT) accounts for the degradation of the impulse response due to the electrical waveform propogating across the radial profile of the sampling beam. In order to calculate the ETT, we assume that all fields are infinitesimal except for the radial profile of the sampling beam. From (3) the impulse response becomes

$$U(\tau)_{\mathrm{ETT}} = I(0, v_y\tau, 0). \tag{9}$$

This time, the beam waist profile in the y direction is mapped as a function of the time delay τ. If we assume a lowest order Gaussian mode with spot size $2w$, the impulse response can be written

$$U(\tau)_{\mathrm{ETT}} = \exp\left(-\frac{2c^2}{\epsilon_{\mathrm{eff}}w^2}\tau^2\right) \tag{10}$$

where ϵ_{eff} is the effective dielectric constant of the transmission line. The pulse width at half maximum is

$$\Delta\tau_{\mathrm{ETT}} = \frac{w}{c}\sqrt{2\ln 2\epsilon_{\mathrm{eff}}} \tag{11}$$

and, by applying a Fourier transform, we obtain a Gaussian frequency response with -3 dB bandwidth

$$f_{-3\mathrm{dB}_{\mathrm{ETT}}} = \sqrt{\frac{\ln 2}{\epsilon_{\mathrm{eff}}}}\frac{c}{\pi w}. \tag{12}$$

C. Optical Pulsewidth Limit

The effect of using a finite time width sampling pulse on the system resolution is intuitively obvious. The time duration of the sampling pulse is a finite "window" through which all field measurements are made. Again, if we assume all dimensions shrink to infinitesimal values and apply the sifting property to (3), the impulse response due to a finite optical pulsewidth (OPW) is

$$U(\tau)_{\mathrm{OPW}} = I(-v_x\tau, 0, 0). \tag{13}$$

As expected, the optical envelope is mapped out via the time delay τ. For a Gaussian time waveform with pulsewidth τ_0 (FWHM) the impulse response is

$$U(\tau)_{\mathrm{OPW}} = \exp\left(-4\ln 2(\tau/\tau_0)^2\right). \tag{14}$$

Transformation to the frequency domain yields a system bandwidth of

$$f_{-3\mathrm{dB}_{\mathrm{OPW}}} = \frac{0.441}{\tau_0} \tag{15}$$

There is an interesting consequence of using the same laser pulse to drive the photodiode as well as to measure its response. We saw that the sampling system impulse response was a cross correlation between the spatial profiles of the traveling electric fields and the sampling optical fields. When the transmission line is driven by a photodiode, the voltage on the line is the convolution between the excitation pulse $I(t)$ and the photodiode impulse response $h(t)$. Thus, we can write the sampler output signal as

$$V(t) = I(t) \star [I(t) * h(t)] \tag{16}$$

where $\star$ indicates cross correlation and $*$ indicates convolution. Since the operations of convolution and correlation are associative [25], we can rewrite (16) as

$$V(t) = [I(t) \star I(t)] * h(t). \tag{17}$$

Hence, we find that the system response is given by the convolution of the autocorrelation function of the laser pulse $[I(t) \star I(t)]$ with the photodiode impulse response. Since we have an independent method of measuring the autocorrelation function using second harmonic generation [26], we can deconvolve the contribution of the optical pulse width. The deconvolution can easily be carried out using Fourier transform techniques; however, noise will be introduced into the calculation at very high frequencies where both the measured waveform spectrum and the autocorrelation spectrum have rolled off considerably.

D. Practical Resolution Limitations

We can now calculate the transit times in the sampling system for a typical microstrip transmission line on a GaAs MMIC. Using the parameters

$$\begin{aligned} h &= 100\ \mu\mathrm{m} && \text{(substrate thickness)} \\ w &= 5\ \mu\mathrm{m} && \text{(beam radius)} \\ n &= 3.5 && \text{(optical index)} \\ \epsilon_{\mathrm{eff}} &\approx 9 && \text{(effective dielectric constant)} \end{aligned} \tag{18}$$

we obtain the following resolution limits:

$$\begin{aligned} \Delta\tau_{\mathrm{OTT}} &= 2.3\ \mathrm{ps} & f_{-3\mathrm{dB}_{\mathrm{OTT}}} &= 190\ \mathrm{GHz} \\ \Delta\tau_{\mathrm{ETT}} &= 60\ \mathrm{fs} & f_{-3\mathrm{dB}_{\mathrm{ETT}}} &= 5.3\ \mathrm{THz}. \end{aligned} \tag{19}$$

The optical transit time effect dominates because of the high index of GaAs and the double pass through the substrate.

In principle, there is a way to reduce or eliminate the transit time effects. If a component of the microwave group velocity can be matched with a similar component of the sampling beam, at least one of the transit times can be eliminated [8]. In Fig. 4, if we tilt the sampling beam with respect to the transmission line, the y-component of the group velocities can be matched and the optical transit time effect disappears. This technique is effective in the transverse $LiTaO_3$ sampler but in GaAs the microwave and optical velocities are nearly the same and the sampling beam would have to be tilted below the critical angle, thus pre-

where, for convenience, we assume the device produces a sinusoidal signal at a frequency ω_m. V_0 is the peak voltage on the line and m is the modulation index. Notice that this is an asymmetrical driving function; the deviation from static retardation

$$\Delta\Gamma = \pi \frac{V(t)}{V_\pi} \tag{31}$$

is positive only.

Combining (29)-(31) we can write the total photocurrent as

$$i_{\text{total}} = \frac{i_0}{2}\left[1 - \cos\Gamma_0 + \pi\frac{V_0}{V_\pi}\left(1 - m\sin^2\frac{\omega_m}{2}t\right)\sin\Gamma_0\right]. \tag{32}$$

By expanding the $\sin^2$ term, we can separate out the average term and the time varying term since they contribute to the received noise power and signal power, respectively.

$$i_{\text{avg}} = \frac{i_0}{2}\left[1 - \cos\Gamma_0 + \pi\frac{V_0}{V_\pi}\left(1 - \frac{m}{2}\right)\sin\Gamma_0\right] \tag{33}$$

$$i_{\text{sig}} = m\frac{i_0}{4}\pi\frac{V_0}{V_\pi}\cos\omega_m t\sin\Gamma_0. \tag{34}$$

If we assume that the modulation index is maximum ($m = 1$), then the mean-square shot noise current density is

$$\overline{i_{SN}^2} = 2qi_{\text{avg}} = qi_0\left(1 - \cos\Gamma_0 + \frac{\pi}{2}\frac{V_0}{V_\pi}\sin\Gamma_0\right) \tag{35}$$

and the mean-square signal current is

$$\overline{i_{\text{sig}}^2} = \frac{i_0^2}{32}\left(\frac{\pi V_0}{V_\pi}\right)^2\sin^2\Gamma_0. \tag{36}$$

We can now write the signal-to-noise ratio as

$$S/N = \frac{i_0^2}{32qB}\left(\frac{\pi V_0}{V_\pi}\right)^2 \cdot \frac{\sin^2\Gamma_0}{i_0\left(1 - \cos\Gamma_0 + \frac{\pi}{2}\frac{V_0}{V_\pi}\sin\Gamma_0\right) + 4kT/qR_L}. \tag{37}$$

We have purposely left the static retardation Γ_0 as a free parameter in this equation so that we may study its effect on the signal-to-noise ratio [27]. Fig. 6 displays (37) plotted as a function of Γ_0 with various values of R_L from 1 Ω to 10K Ω including $R_L \to \infty$. We see that when shot noise dominates ($R_L \to \infty$), the signal-to-noise ratio improves by a factor of two as $\Gamma_0 \to 0$ compared to operating at the quarter-wave bias point $\Gamma_0 = \pi/2$. However, as Γ_0 is reduced, so is the signal. If a finite load resistance is included, at some point the Johnson noise will be comparable with the signal and the signal-to-noise ratio will reduce as Γ_0 is reduced. This trend is evident in Fig. 6.

The factor $\pi V_0/2V_\pi \sin\Gamma_0$ in the denominator of (37)

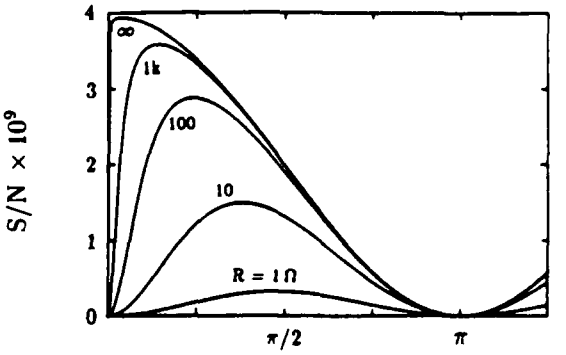

Fig. 6. Signal-to-noise ratio versus static phase retardation Γ_0 for various photodiode load resistances. Curves are drawn for GaAs assuming 1 V on the transmission line, a maximum receiver photocurrent of 20 mA and a bandwidth of 1 Hz.

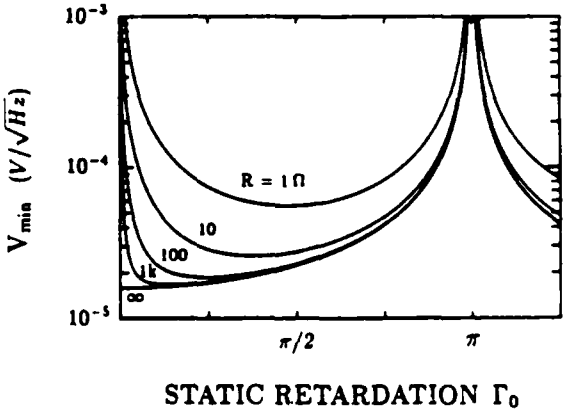

Fig. 7. Minimum detectable voltage V_{min} versus static retardation Γ_0 for the same load resistances as in Fig. 6. Curves are drawn for GaAs assuming a maximum receiver photocurrent of 20 mA and a bandwidth of 1 Hz.

arises as a contribution to the average current (and hence the shot noise) because of the asymmetrical modulation of the transmission line waveform (i.e., the voltage on the transmission line is always positive so the average optical power is increased). The magnitude of this term is only significant for very large values of V_0/V_π ($\geq 10^{-3}$) and then it only makes a difference for very small values of Γ_0. Calculations show that when V_0/V_π is increased from 10^{-4} to 10^{-1}, the coefficient to the right of $(V_0/V_\pi)^2$ in (37) is reduced by half. However, the total signal-to-noise ratio has increased by 0.5×10^6 and, hence, this effect can be neglected (recall that for typical signals, $V_0 \ll V_\pi$).

With this approximation in mind, we set (37) equal to one and solve for voltage V_{min} which represents the minimum detectable voltage (normalized to 1 Hz bandwidth).

$$V_{\text{min}} = \frac{8}{i_0}\frac{V_\pi}{\pi}\sqrt{q\frac{i_0\sin^2\Gamma_0/2 + 2kT/qR_L}{\sin^2\Gamma_0}} \quad V/\sqrt{Hz}. \tag{38}$$

It is interesting to explore the variation in the minimum detectable voltage with Γ_0. This is presented in Fig. 7 where V_{min} is plotted versus Γ_0 for the same load resis-

where d is the beam diameter and ϵ is the dielectric permittivity. In our sampling geometry where the probe beam enters through the top of the (100) grown GaAs wafer and reflects off the ground plane, d is replaced by the substrate thickness h and (46) becomes

$$V_i(t) = \frac{n^3 r_{41} h}{\epsilon c} I(t) \tag{47}$$

where $I(t)$ is the intensity envelope of the sampling pulse. For simplicity, we assume $I(t)$ is triangular in shape with pulsewidth τ and peak value I_0. Solving (45) with (47) as the driving function results in a peak voltage

$$V_0(0) = \frac{n^3 r_{41} h}{\epsilon c} I_0 \frac{RC}{\tau} [1 - \exp(-\tau/RC)] \tag{48}$$

appearing on the transmission line. Thus, using the following parameters appropriate for a 100 μm thick GaAs MMIC

$$r_{41} = 1.2 \times 10^{-12} \text{ m/V}$$
$$n = 3.44$$
$$d = 10 \ \mu\text{m}$$
$$\epsilon = 12.3 \times \epsilon_0$$
$$I_0 = 6.4 \times 10^7 \text{ W/cm}^2$$
$$RC = 2.1 \text{ fs}$$
$$\tau = 5 \text{ ps}$$
$$h = 100 \ \mu\text{m}$$

we calculate a peak voltage of

$$V_0(0) = 41 \ \mu\text{V}.$$

This is very small compared to typical voltages to be measured in the electrooptic sampler, yet it is comparable to the minimum detectable voltage in a 1 Hz receiver bandwidth. It is interesting to note that this signal is being produced at the same rate as the sampling pulses and if the waveform being measured has a chopping-frequency component, then the optical rectification signal will never be detected.

In spite of the weak effect, optical rectification from femtosecond pulses is currently being investigated as a source of far-infrared radiation for transient spectroscopy in a series of elegant experiments by Auston *et al.* [30] and Cheung and Auston [31].

V. Electrooptic Sampling in GaAs

A. Electrooptic Effect in GaAs

Gallium arsenide belongs to the cubic zincblende group with crystal symmetry $\bar{4}3m$. The electrooptic tensor for this group has the form

$$r_{mk} = \begin{pmatrix} 0 & 0 & 0 \\ 0 & 0 & 0 \\ 0 & 0 & 0 \\ r_{41} & 0 & 0 \\ 0 & r_{41} & 0 \\ 0 & 0 & r_{41} \end{pmatrix} \tag{49}$$

When an electric field is applied to the crystal, a birefringence is induced and the initially spherical index ellipsoid is distorted. The intersection of the index ellipsoid and a plane normal to the direction of optical propagation defines an ellipse whose major and minor axes give the allowed polarization directions and the associated indices of refraction. For GaAs, the ellipsoid is described by

$$\frac{x^2 + y^2 + z^2}{n_0^2} + 2r_{41}(E_x yz + E_y zx + E_z xy) = 1 \tag{50}$$

where x, y, and z are parallel to the crystallographic axes [100], [010], and [001], respectively.

The most common orientation for GaAs wafers in the integrated circuits industry is (100) (i.e., the normal to the wafer surface is in the [100] direction) [32]. Since the most convenient geometry for optical probing is one in which the beam enters the wafer normal to its surface, we investigate the index ellipse for [100] propagation. In the $x = 0$ plane, we have

$$\frac{y^2 + z^2}{n_0^2} + 2r_{41} E_x yz = 1 \tag{51}$$

which has principal axes y' and z' at 45° with respect to y and z and corresponding indexes [33]

$$n_y' = n_0 + \tfrac{1}{2} n_0^3 r_{41} E_x$$
$$n_z' = n_0 - \tfrac{1}{2} n_0^3 r_{41} E_x. \tag{52}$$

Note that for light incident along x, only the x component of the applied electric field contributes to the induced birefringence. Thus, for an arbitrary electric field distribution in a (100) wafer of GaAs, the single pass phase retardation is given by

$$\Gamma = \frac{2\pi}{\lambda} n_0^3 r_{41} V_{12} \tag{53}$$

where V_{12} is the potential difference between the front and back side of the wafer. For the microstrip transmission line geometry of Fig. 1(b), a focused beam of light which enters the GaAs wafer at a point adjacent to the top conductor and reflects from the ground plane experiences a round trip retardation of

$$\Gamma = \frac{4\pi}{\lambda} n_0^3 r_{41} V \tag{54}$$

where V is the potential of the top conductor.

For light propagating along x, the result of (53) is com-

beam (Fig. 10). Because the excitation pulses were derived from the sampling beam, this method is free from timing jitter.

D. Experimental Results

1) GaAs Reflectance Modulator: The first step toward demonstrating a high speed sampling system in GaAs was to demonstrate a basic low-frequency electrooptic modulator [44]–[46]. Choosing the longitudinal interaction geometry as a test case, a simple reflectance modulator was constructed in order to verify the sensitivity of the fringing field interaction.

At 1.5 mw HeNe laser operating at 1.15 μm was used as the infrared source. The linearly polarized output was converted to circular polarization with a Soliel–Babinet compensator adjusted for quarter wave retardation. The beam was focused with a standard 5× microscope objective onto a GaAs wafer adjacent to a microstrip transmission line where it entered the crystal and reflected off the ground plane on the back side. After the beam exited the crystal, the microscope objective recollimated it parallel to the incident beam and slightly displaced where a mirror directed it to the analyzer and photodiode. The transmission line was driven with a sine wave generator with 1 V peak-to-peak amplitude at a frequency of 1 kHz.

Taking into account the 30 percent Fresnel reflection of the incident light from the surface of the GaAs, we measured a half-wave switching voltage of 10.5 kV. This is a factor of two high and the error may have to do with the nature of the distribution of the fringing fields (i.e., the potential is lower immediately adjacent to the transmission lines). Also, if a large spot size is used and is centered on the fringing field, some of the beam might be reflected by the top conductor of the transmission line, reducing the electrooptic interaction.

As the optical beam was moved away from the transmission line, the signal diminished as expected due to the local confinement of the electric fields. However, when an additional visible HeNe laser (λ = 632 nm) was used to flood-illuminate the surface of the GaAs in the vicinity of the sampling beam, the signal returned to its original value. This suggests that a conductive surface is being photogenerated and that charge from the transmission line is accumulating there, reestablishing an electric field in the sampling beam. The photoconductive surface may play an important role in future measurements because it can be used to optically alter, or introduce, new conductive patterns on any GaAs wafer. This might be useful for introducing known reflections as timing markers in time domain reflectometry measurements, or, as a way of rapidly designing new transmission-line structures without intermediate processing steps.

2) Photodiode Characterization: In this experiment, we measured the impulse response of a GaAs photodiode that was excited by the second harmonic of the sampling beam [10]. Although the photodiode made a hybrid connection to the GaAs microstrip transmission line, the principle of excitation and sampling of an active GaAs device was demonstrated.

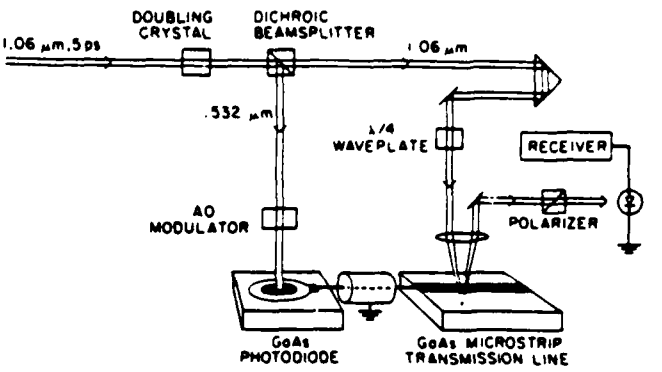

Fig. 11. Schematic diagram of an electrooptic sampling system for direct probing in GaAs substrates.

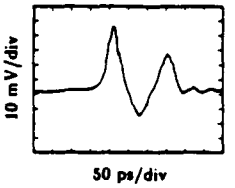

Fig. 12. Impulse response of a 50 μm diameter GaAs photodiode measured by electrooptic sampling of a GaAs microstrip transmission line (horizontal: 50 ps/div; vertical: ≈ 10 mV/div).

The experimental set up is indicated schematically in Fig. 11. It functions in an identical manner to the apparatus shown in Fig. 3, but with a different optical source. Instead of a synchronously pumped dye laser, we used a Spectra-Physics model 3000 Nd : YAG laser in conjunction with a model 3600 pulse compressor to produce a train of 5 ps pulses at a rate of 82 MHz. The doubling crystal was KTP and an acoustooptic modulator was used to chop the excitation beam at 20.9 MHz. Fig. 12 shows the impulse response of a 50 μm diameter GaAs Schottky photodiode [47] measured with this system.

3) MMIC Testing: The real power and flexibility of our sampling approach can be demonstrated best when applied to measurements made in complex integrated circuits. Weingarten and Rodwell have sampled the output of a four stage GaAs FET traveling wave amplifier (TWA, courtesy of G. Zdasiuk, Varian Associates), measuring electronic distortion induced by changes in the power supply bias [11], [48]. In this experiment, instead of driving the device under test with a photodiode, it was connected to a microwave synthesizer (HP 8340A), phase-locked to the laser mode-locker driver and operating at a fixed frequency. The frequency was chosen to be an exact multiple of the fundamental sampling rate plus 1 Hz so that the sampling pulses walked through the driving sinusoid at a rate of 1 Hz. Pulse modulating the synthesizer at 10 MHz, allowed a narrow-band receiver to be used for signal-to-noise enhancement. Since the spectrum analyzer used as the 10 MHz receiver displayed only the rms value of the sampled waveform a small amount of the 10 MHz chopping signal was injected into the input so that it summed vectorially with the photodiode signal to produce a true bipolar waveform.

With the synthesizer tuned to 4.1 GHz and the TWA

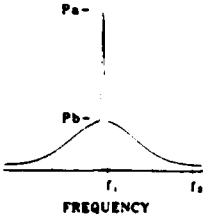

Fig. 16. Typical laser envelope harmonic spectral component. P_a = carrier power, P_b = phase noise power at any offset from the carrier. (See text for explanation of f_1 and f_2.)

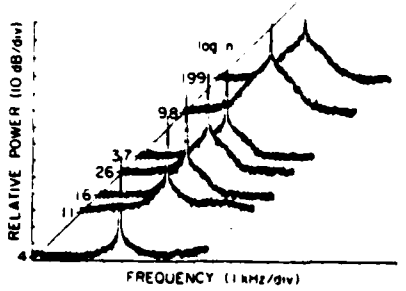

Fig. 17. Laser envelope harmonic spectral components down-converted to 10 MHz by harmonic mixing in the electrooptic sampler. Center frequency of each component equals $n \times 82$ MHz, where n is the harmonic number.

16. It consists of a delta function at nf_0 and a phase noise pedestal arising from the pulse-to-pulse jitter. For small phase fluctuations, the relative phase noise power can be shown to vary as the square of the harmonic number n [50]. The phase noise-to-carrier power ratio for a given sinusoidal component of the noise is given by

$$\frac{P_b}{P_a} = \frac{(n\omega_0\tau_0)^2}{2} \tag{55}$$

where

P_b = phase noise power at some offset frequency

P_a = carrier power

$\omega_0 = 2\pi \times$ sampling rate

τ_0 = peak timing jitter at frequency of P_b.

Fig. 17 shows a series of harmonic spectra from the mode-locked and compressed Nd : YAG laser mixed down to 10 MHz. To obtain these spectra, signals up to 16 GHz (n = 199) were applied to the transmission line from a microwave synthesizer (HP 8340A) that was phase-locked to the mode-locker driver (HP 3325A). The growth of the phase noise sidebands is clearly evident. By measuring the relative intensity of the phase noise and plotting it against the actual frequency of the harmonic (nf_0), the rate of sideband growth can be compared to the theory. In Fig. 18, these data are plotted on a log–log graph against a slope = 2 line. The data follow the square-law dependence well with the deviation at the high end assumed to result from the higher modulation index causing a nonlinear departure from the small-signal theory.

With a picture of one of the spectral components in

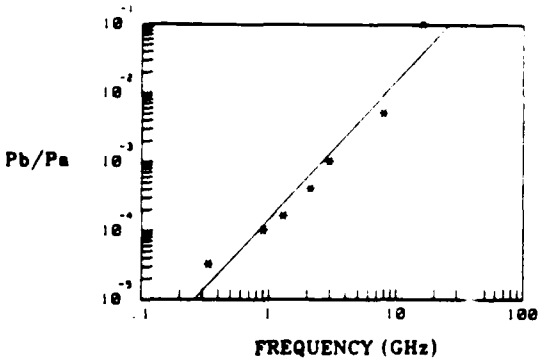

Fig. 18. Relative growth of phase noise power as a function of harmonic frequency ($n \times 82$ MHz). Solid line of slope = 2 corresponds to theoretical square-law dependence.

hand, we can deduce the extent of the timing fluctuations because the total power in the phase noise sidebands, P_{DSB}, can be shown to be related to the rms timing jitter [50], [51]. To calculate the total double side-band noise power, the phase noise spectrum is integrated from some low frequency f_1 near the carrier (nf_0) to some higher frequency f_2 where the phase noise falls to the level of the AM and Johnson noise. Since the apparent width of the carrier component depends on the resolution bandwidth of the spectrum analyzer, using a narrower bandwidth allows f_1 to move closer to the carrier and lower frequency phase fluctuations to contribute to the total side-band power. Thus, any calculation of timing jitter using this method must specify the low frequency cutoff f_1. The expression relating the rms timing jitter to the carrier and phase noise powers is

$$\Delta t_{rms} = \frac{T}{2\pi n}\sqrt{\frac{P_{DSB}}{P_a}} \tag{56}$$

where

$$P_{DSB} = 2\int_{f_1}^{f_2} \frac{P_b(f)}{B}\,df \tag{57}$$

and B = spectrum analyzer resolution bandwidth and $T = 1/f_0$.

In our experiments we used two spectrum analyzer bandwidth settings. In the first case with the bandwidth B = 10 Hz, the low-frequency cutoff f_1 ranged between 10 Hz and 32 Hz. In the second case, B = 30 Hz and f_1 varied from 105 Hz to 150 Hz. The upper frequency limit f_2 was typically 1 kHz–2 kHz.

The rms timing jitter calculated from the phase noise spectra and (56) is plotted in Fig. 19 for five harmonic components from n = 11 to n = 98. Although there is a spread of several picoseconds in the jitter for each of the two resolution bandwidths, the slopes connecting the two data points of each harmonic number are nearly the same, indicating a similar trend in increasing jitter as lower frequency components are included. The data suggest an upper limit of 11 ps rms jitter for fluctuation frequencies above 10 Hz. We have not yet identified the source of the

[15] G. A. Mourou and K. E. Meyer, "Subpicosecond electro-optic sampling using coplanar strip transmission lines," *Appl. Phys. Lett.*, vol. 45, pp. 492–494, 1984.
[16] R. E. Collin, *Foundations for Microwave Engineering*. New York: McGraw-Hill, 1966.
[17] K. E. Meyer and G. A. Mourou, "Two-dimensional E-field mapping with subpicosecond resolution," in *Topical Meeting on Picosecond Electronics and Optoelectronics, Technical Digest*, Mar. 1985, paper WB3-1. New York: Springer-Verlag, 1985.
[18] J. D. Kafka, B. H. Kolner, T. Baer, and D. M. Bloom, "Compression of pulses from a continuous-wave mode-locked Nd:YAG laser," *Opt. Lett.*, vol. 9, pp. 505–506, 1984.
[19] B. H. Kolner, J. D. Kafka, D. M. Bloom, and T. M. Baer, "Compression of mode-locked Nd:YAG pulses to 1.8 ps," in *Ultrafast Phenomena IV*. New York: Springer-Verlag, 1984.
[20] J. P. Heritage, R. N. Thurston, W. J. Tomlinson, A. M. Weiner, and R. H. Stolen, "Spectral windowing of frequency modulated optical pulses in a grating compressor," *Appl. Phys. Lett.*, vol. 47, pp. 87–89, 1985.
[21] A. S. L. Gomes, W. Sibbett, and J. R. Taylor, "Generation of subpicosecond pulses from a continuous-wave mode-locked Nd:YAG laser using a two-stage optical compression technique," *Opt. Lett.*, vol. 10, pp. 338–340, 1985.
[22] I. P. Kaminow, *An Introduction to Electrooptic Devices*. New York: Academic, 1974.
[23] J. F. Nye, *Physical Properties of Crystals*. Oxford, England: Oxford University Press, 1979.
[24] B. H. Kolner, "Picosecond electro-optic sampling in GaAs," Ph.D. dissertation, Stanford Univ., Stanford, CA, 1985.
[25] R. N. Bracewell, *The Fourier Transform and its Applications*. New York: McGraw-Hill, 1978.
[26] E. P. Ippen and C. V. Shank, "Techniques for measurement," in *Ultra-short Light Pulses*, S. L. Shapiro, Ed. New York: Springer-Verlag, 1977, pp. 83–122.
[27] S. Williamson and G. Mourou, "Picosecond electro-electron oscilloscope," in *Topical Meet. Picosecond Electron. Optoelectron., Tech. Dig.*, Mar. 1985, postdeadline paper PDP2.
[28] Y. R. Shen, *The Principles of Nonlinear Optics*. New York: Wiley, 1984.
[29] J. F. Ward, "Absolute measurement of an optical-rectification coefficient in ammonium dihydrogen phosphate," *Phys. Rev.*, vol. 143, pp. 569–574, 1966.
[30] D. H. Auston, K. P. Cheung, J. A. Valdmanis, and D. A. Kleinman, "Cherenkov radiation from femtosecond optical pulses in electro-optic media," *Phys. Rev. Lett.*, vol. 53, pp. 1555–1558, 1984.
[31] K. P. Cheung and D. H. Auston, "Distortion of ultrashort pulses on total internal reflection," *Opt. Lett.*, vol. 10, pp. 218–219, 1985.
[32] R. E. Williams, *Gallium Arsenide Processing Techniques*. Dedham, MA: Artech House, 1984.
[33] Susumu Namba, "Electro-optical effect of zincblende," *J. Opt. Soc. Amer.*, vol. 51, pp. 76–79, 1961.
[34] J. L. Freeman, Jr., S. K. Diamond, H. Fong, and D. M. Bloom, "Electro-optic sampling of planar digital GaAs integrated circuits," *Appl. Phys. Lett.*, vol. 47, pp. 1083–1084, 1985.
[35] R. L. Fork, Charles V. Shank, R. Yen, and C. A. Hirlimann, "Femtosecond optical pulses," *IEEE J. Quantum Electron.*, vol. QE-19, pp. 500–506, 1983.
[36] J. A. Valdmanis, R. L. Fork, and J. P. Gordon, "Generation of optical pulses as short as 27 femtoseconds directly from a laser balancing self-phase modulation, group velocity dispersion, saturable absorption and saturable gain," *Opt. Lett.*, vol. 10, pp. 131–133, 1985.
[37] L. F. Mollenauer and D. M. Bloom, "Color-center laser generates picosecond pulses and several watts cw over the 1.24–1.45 μm range," *Opt. Lett.*, vol. 14, pp. 247–249, 1979.
[38] D. Grischkowsky and A. C. Balant, "Optical pulse compression based on enhanced frequency chirping," *Appl. Phys. Lett.*, vol. 41, pp. 1–3, 1982.
[39] B. Nikolaus and D. Grischkowsky, "12 × pulse compression using optical fibers," *Appl. Phys. Lett.*, vol. 42, pp. 1–3, 1983.
[40] C. V. Shank, R. L. Fork, R. Yen, and R. H. Stolen, "Compression of femtosecond optical pulses," *Appl. Phys. Lett.*, vol. 40, pp. 761–763, 1982.
[41] A. M. Johnson, R. H. Stolen, and W. M. Simpson, "80 × single-stage compression of frequency doubled Nd:yttrium aluminum garnet laser pulses," *Appl. Phys. Lett.*, vol. 44, pp. 729–731, 1984.
[42] W. J. Tomlinson, R. H. Stolen, and C. V. Shank, "Compression of optical pulses chirped by self-phase modulation in fibers," *J. Opt. Soc. Amer. B*, vol. 1, pp. 139–149, 1984.
[43] E. B. Treacy, "Compression of picosecond light pulses," *Phys. Lett.*, vol. 28A, pp. 34–35, 1968.
[44] Lily Ho and C. F. Buhrer, "Electro-optic effect of gallium arsenide," *Appl. Opt.*, vol. 2, pp. 647–648, 1963.
[45] A. Yariv, C. A. Mead, and J. V. Parker, "GaAs as an electro-optic modulator at 10.6 microns," *IEEE J. Quantum Electron.*, vol. QE-2, pp. 243–245, 1966.
[46] T. E. Walsh, "Gallium arsenide electro-optic modulators," *RCA Rev.*, vol. 27, pp. 323–335, 1966.
[47] S. Y. Wang, D. M. Bloom, and D. M. Collins, "20-GHz bandwidth GaAs photodiode," *Appl. Phys. Lett.*, vol. 42, pp. 190–192, 1983.
[48] K. J. Weingarten, M. J. W. Rodwell, H. K. Heinrich, B. H. Kolner, and D. M. Bloom, "Direct electro-optic sampling of GaAs circuits," *Electron. Lett.*, vol. 21, pp. 765–766, 1985.
[49] G. D. McCormack, A. G. Rode, and E. W. Strid, "A GaAs MSI 8-bit multiplexer and demultiplexer," in *Proc. 1982 GaAs IC Symp.*, Beaverton, OR, pp. 25–28, courtesy of TriQuint Semiconductor, Inc.
[50] J. Kluge, "Synchronously pumped dye lasers for ultrashort light pulse generation," Ph.D. dissertation, Univ. Essen, Fed. Rep. Germany, 1984.
[51] W. P. Robins, *Phase Noise in Signal Sources*. England: Peregrinus, 1982.
[52] D. Cotter, "Technique for highly stable active mode-locking," in *Ultrafast Phenomena IV*. New York: Springer-Verlag, 1984.

Brian H. Kolner (SM'85) was born in Chicago, IL, on June 22, 1955. He received the B.S. degree in electrical engineering from the University of Wisconsin, Madison, in 1979 and the M.S. and Ph.D. degrees in electrical engineering from Stanford University, Stanford, CA, in 1981 and 1985, respectively.

From 1979 to 1983 he was a part-time employee with Hewlett-Packard Laboratories, Palo Alto, CA, where he worked on surface acoustic wave devices, integrated optical directional coupler modulators, and electrooptic sampling. He has also collaborated with Spectra-Physics Corporation and Bell Communications Research. In 1985 he rejoined the Staff at Hewlett-Packard Laboratories where his current interests include high-speed electronic and optoelectronic devices, electrooptic sampling, optical pulse compression, and ultrafast phenomena.

Dr. Kolner is a member of the Optical Society of America.

David M. Bloom (S'68–M'76–M'80) was born on October 10, 1948 in Brooklyn, NY. He received the B.S. degree in electrical engineering from the University of California, Santa Barbara, in 1970 and the M.S. and the Ph.D. degrees in electrical engineering from Stanford University, Stanford, CA, in 1972 and 1975, respectively.

From 1975 to 1977 he was employed by Stanford University as a Research Associate. During this period he was awarded the IBM Postdoctoral Fellowship. From 1977 to 1979 he was employed by Bell Telephone Laboratories, Holmdel, NJ, where he conducted research on optical phase conjugation, ultrafast optical pulse propagation in fibers, and tunable color-center lasers. From 1979 to 1983 he served on the Staff and later as a Project Manager at Hewlett Packard Laboratories, Palo Alto, CA. While there he conducted and managed research on fiber optical devices, high-speed photodetectors, and picosecond electronic measurement techniques. In late 1983 he joined the Edward L. Ginzton laboratory, W. W. Hansen Laboratories of Physics, Stanford University, where he is currently an Associate Professor of Electrical Engineering. His current research interests are ultrafast optics and electronics.

Dr. Bloom was awarded the 1980 Adolph Lomb Medal of the Optical Society of America for his pioneering work on the use of nonlinear optical processes to achieve real time conjugate wavefront generation. In 1981 he was elected a Fellow of the Optical Society of America in recognition of his distinguished service in the advancement of optics. He is the 1985 IEEE LEOS Travelling Lecturer.

Gate Propagation Delay and Logic Timing of GaAs Integrated Circuits Measured by Electro-Optic Sampling

M.J.W. Rodwell, K.J. Weingarten, J.L. Freeman,
and D.M. Bloom

Edward L. Ginzton Laboratory
Stanford University
Stanford, CA 94305, USA

Abstract: We report techniques for measuring internal switching delays of GaAs digital integrated circuits by electro-optic sampling. Circuit propagation delays of 15 ps are measured. A new phase modulation technique which allows testing of sequential logic is demonstrated with the measurement of a 2.7 GHz 8-phase clock generator.

Submitted to Electronics Letters.

We have used the system to measure the edgespeed and propagation delays of GaAs buffered FET logic (BFL) combinational logic. To accurately measure the transition times and the shape of the switching waveforms, the impulse response of the sampling system must be short and free of "wings" (long duration substructure), which would introduce tilt into the measured waveforms. By using 1 km fibre in the pulse compressor, significant group velocity dispersion is introduced, producing a more linear frequency chirp; the resulting compressed pulses are of 2 ps duration and are free of wings [6], giving a Fourier transform 3 dB frequency of 100 GHz . Other time resolution limitations, including the optical transit time [4] and the 2 ps laser timing jitter, further limit the bandwidth to about 70 GHz.

Laser timing drift can cause errors in gate propagation delay measurements. The laser timing stabilizer reduces this drift to about 1 ps/minute. Automated positioners are used to scan rapidly between probed points, reducing the drift bet4ween measurements to less than 1 ps.

To acquire measurements rapidly requires low instrument noise. In addition to shot noise, the laser has 80 dB excess low-frequency amplitude noise, while the compressor generates excess amplitude noise which is correlated to Raman scattering in the fibre. In contrast to shorter fibres, with the 1 km fibre we attain 50X pulse compression at power levels below the threshold of the Raman process. This occurs because self phase modulation occurs over the entire length of the fibre while the interaction

use a small-deviation phase modulator driven at 10 MHz. The photocurrent received then has a component at 10 MHz proportional to the derivative of the sampled point on the circuit waveform. The receiver detects and integrates the 10 MHz component to reconstruct the waveform. The phase modulation must be less than 1 radian of the highest waveform harmonic of interest if less than 1 dB of attenuation of this harmonic is to be incurred. Because of this limitation, and because of the signal integration, measurement noise is increased, being proportional to the square of the number of recovered harmonics, rather than in direct proportion. Acquisition times are on the order of 1 second.

We have used the phase modulation technique to probe the 8-phase counter/clock generator waveforms in a GaAs BFL 8-bit multiplexer/demultiplexer [8] clocked at 2.7 GHz (fig. 3). Because the multiplexer cycles on both the rising and falling edges of (in this case) an assymmetrical input clock, the 8 phases of the counter are unevenly timed.

In conclusion, we have used electro-optic sampling to measure propagation delays and timing of GaAs logic. The sampler, whose bandwidth we estimate at 70 GHz, has been used to sample signals as high in frequency as 40 GHz (fig. 4); thus risetimes as small as 5 ps can be resolved. The external synchronisation and phase modulation techniques allow accurate testing of combinational and sequential logic with the circuits operating in their normal mode, being driven with complex repetitive digital sequences.

4. Kolner, B.H. and Bloom, D.M.: "Electro-Optic Sampling in GaAs Integrated Circuits", ibid.,vol. QE-22, Jan. 1986, pp. 79-93

5. Kafka, J.D., Kolner, B.H., Baer, T., and Bloom, D.M.: "Compression of pulses from a continuous-wave mode-locked Nd:YAG laser", Opt. Lett., 1984,9, pp. 505-506

6. Grischowsky, D. and Balant, A.C.: "Optical pulse compression based on enhanced frequency chirping", Appl. Phys. Lett., 1982, 41, pp. 1-2

7. Swierkowski, S., Mayeda, K., Cooper, G. and McGonaghy, C.: " A Sub-200 Picosecond GaAs Sample-and-Hold Circuit for a Multi-Gigasample/Second Integrated Circuit" in Tech. Digest, 1985 International Electron Devices Meeting, pp. 272-275 : Dec. 1985.

8. McCormack, G.D., Rode, A.G., Strid, E.W.: " A GaAs MSI 8-bit Multiplexer and Demultiplexer", Proc. 1982 GaAs IC Symposium, pp. 25-28: Nov. 1982.

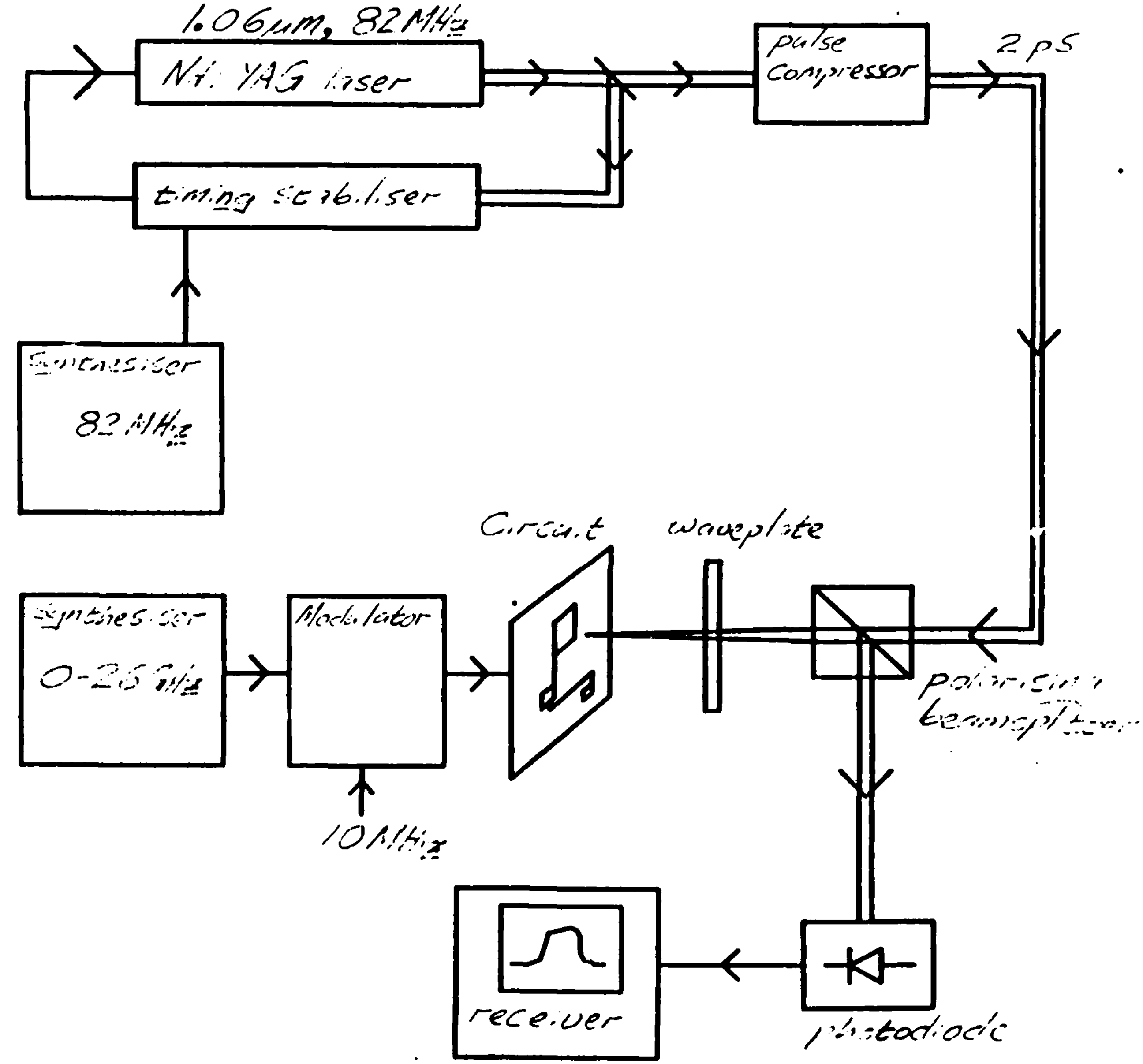

1.06μm, 82MHz
Nd: YAG laser
timing stabiliser
pulse compressor
2 ps
82 MHz
Modulator
0-26 GHz
10 MHz
Circuit
waveplate
receiver
photodiode

FIGURE 3

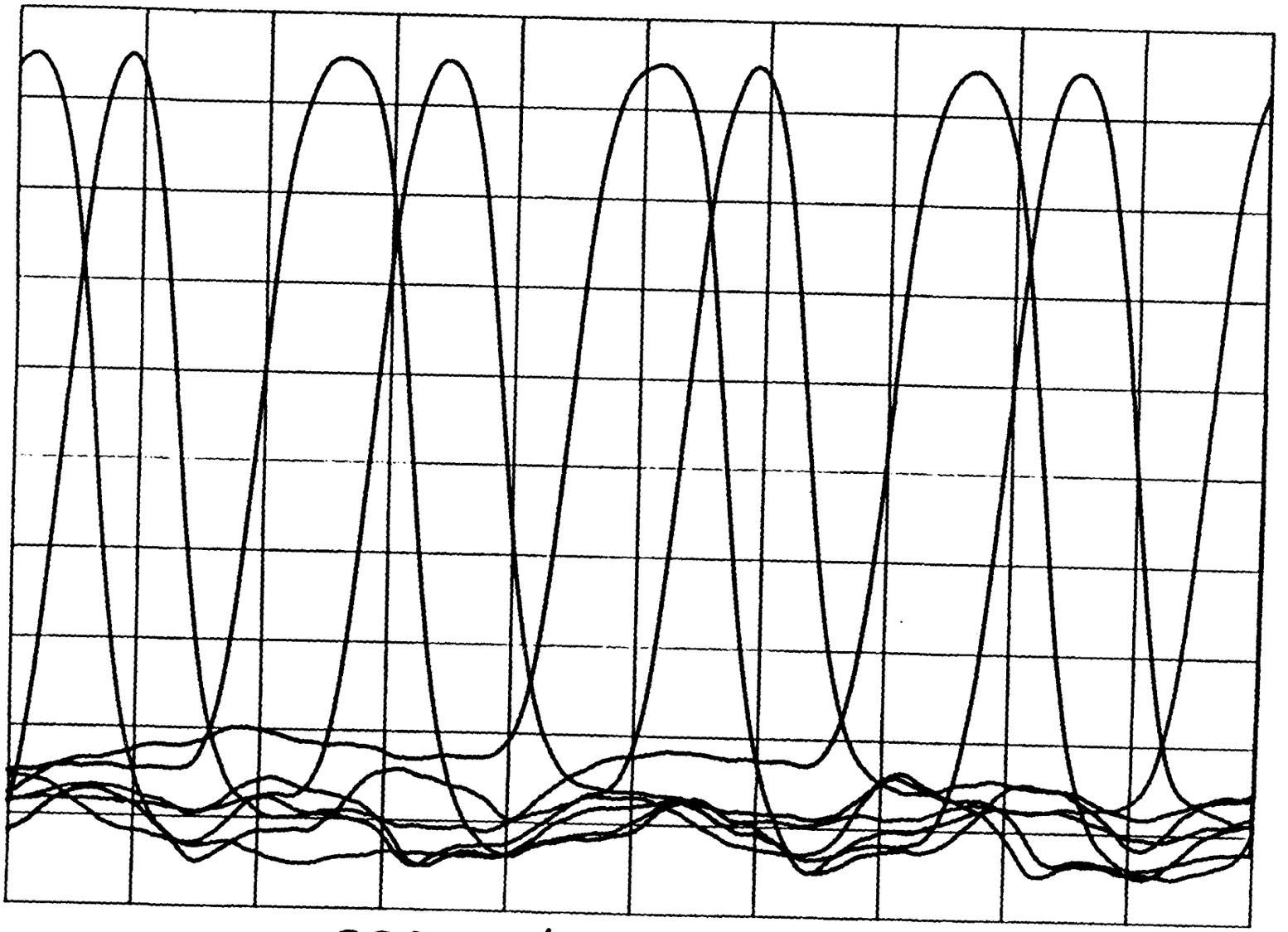

300 ps/division

Internal Microwave Propagation and Distortion Characteristics of Travelling-Wave Amplifiers Studied by Electro-Optic Sampling

M.J.W. Rodwell, M. Riaziat* , K.J. Weingarten, B. A. Auld and D.M. Bloom

Stanford University, Edward L. Ginzton Laboratory
Stanford, California, 94305

*Varian Research Center, 611 Hansen Way, Palo Alto, California, 94303

Abstract

The internal signal propagation and saturation characteristics of two monolithic microwave travelling-wave amplifiers (TWA) are measured by electro-optic sampling. Gate and drain-line responses are compared with theory and simulation, leading to revisions in the FET models. Drain voltage frequency dependence and harmonic current propagation together lead to more complex saturation behavior than is discussed in the literature.

To be published in the 1986 MTT Conference Journal

measuring the voltage on microstrip and coplanar transmission lines are shown in figures 1 and 2, respectively.

Figure 3 shows the sampling system. A mode-locked Nd:YAG laser is driven at 82 MHz, producing optical pulses of 1.06 μm wavelength and 100 ps duration. A fiber-grating pulse compressor reduces the pulse duration to 2 ps and a phase-lock-loop feedback timing stabilizer reduces the laser timing jitter to 2 ps. The probe beam passes through a polarizing beamsplitter and a waveplate and is focused adjacent to or on the conductor of interest for the microstrip or coplanar geometries, respectively. The reflected light passes back through the polarizing beamsplitter, where one polarization is directed onto a photodiode connected to a receiver.

The circuit under test is driven by a microwave synthesizer whose output is pulse modulated at 10 MHz to allow synchronous detection at this frequency. If the microwave synthesizer is tuned to exactly the Nth harmonic of the laser pulse repetition frequency, the same point on the circuit waveform will be sampled every N cycles. The microwave frequency is then offset 10-100 Hz to map out the waveform at this rate. In this way the sampler operates as a sampling oscilloscope. To use the sampler as a network analyzer, we remove the pulse modulation, offset the microwave frequency by 10 MHz and replace the receiver with a narrowband 10 MHz vector voltmeter. Using the sampler we have investigated the causes of bandlimiting and gain compression in two microwave TWA's.

Amplifiers Tested

In a distributed amplifier, a series of small transistors are connected at regular spacings between two high-impedance transmission lines (Fig. 4). The high-impedance lines and the FET capacitances together form synthetic transmission lines, generally of 50 ohm characteristic impedance. Series stubs are used in the drain circuit, equalizing the phase velocities of the two lines and, at high frequencies, providing partial impedance matching of the drain output impedances and thus increasing the gain. By using small devices at small spacings, the cutoff frequencies due to the periodicities of the synthetic lines can be made larger than the bandwidth limitations associated with the line attenuations arising

in strong frequency dependence of the drain voltages (Fig. 9); this can be predicted by simple analysis.

Drain Voltage Distribution

After Ayasli [7], if the wavelength is much greater than the spacing between the FET's, the synthetic lines can be approximated as continuous structures coupled by a uniformly distributed transconductance. The lines then have characteristic impedances and phase velocities given by the sum of distributed and lumped capacitances and inductances per unit length [7]; the line impedances (Z_o) and velocities (V_p) are generally made equal. The lines then have propagation constants given by:

$$\gamma_g = \alpha_g + j\beta_g \simeq \frac{r_g \omega^2 C_{gs}^2 Z_o}{2l} + j\omega/V_p$$

(1)

$$\gamma_d = \alpha_d + j\beta_d \simeq \frac{Z_o G_{ds}}{2l} + j\omega/V_p$$

(2)

Where l is the FET spacing, C_{gs} is the gate-source capacitance, r_g is the gate resistance, G_{ds} is the drain-source conductance, and a forward propagating wave is of the form $e^{-\gamma z}$. The voltage along the drain line is

$$V_d(z) = \frac{Z_o g_m V_{in}}{2l} e^{-p\gamma_g z} \left\{ \frac{1 - e^{(\gamma_g - \gamma_d)z}}{\gamma_d - \gamma_g} + \frac{1 - e^{(\gamma_g + \gamma_d)(z - nl)}}{\gamma_d + \gamma_g} \right\}$$

(3)

where n is the number of FET's, g_m is the FET transconductance, V_{in} is the input voltage, and z is the distance along the drain line, with the origin located at the drainline reverse termination. Ignoring line attenuation, (3) becomes:

$$\|V_d(z)\| = \frac{Z_o g_m V_{in}}{2l} \sqrt{z^2 + z\frac{sin(2\beta(nl - z))}{\beta} + \frac{sin^2(\beta(nl - z))}{\beta^2}}$$

(4)

and if the drainline reverse termination is omitted and the output load resistance Z_{load} set at:

$$Z_{load} = K/nl$$

(6)

then the voltage along the drain line will be uniform:

$$V_d(z) = -ng_m Z_{load} V_{in} e^{-jwz/V_p}$$

(7)

The drainline voltage is uniform and in phase with the gateline voltage, allowing simultaneous saturation of all FET's and thus maximizing the output power at saturation.

In the uniform drain line case, as is shown by equation (3) and by Figure 5, the reverse wave on the drain line complicates the problem; the drain voltages are equal only at low frequencies, and, by equation (3), the reverse wave introduces a phase shift between the gate and drain voltages of each FET. Thus, in the uniform drain line case, neither the conditions for simultaneous saturation of all FET's nor the conditions for simultaneously reaching all saturation mechanisms in a given FET can be met.

The 2-18 GHz microstrip amplifier has 1 dB gain compression at 7 dBm input power, and is not optimized for maximum power output; the lines are not tapered and the bias is such that drain saturation occurs first. At 3 GHz, the small-signal voltages at the drains of the last three devices are approximately equal, thus clipping occurs simultaneously at these three devices (Fig. 13).

At 10 GHz the distortion at the 1 dB compression point is complicated by phase shifts between the 10 GHz fundamental and the 20 GHz generated harmonic currents (Fig. 14). The 10 GHz small-signal voltage at drain 5 is 1.5 dB larger than that at drain 4, thus FET 5 saturates more strongly. The 20 GHz harmonic current generated at FET 5 produces equal forward and reverse drain voltage waves at 20 GHz. With 10 ps line delay between drains 4 and 5, the 20 GHz reverse wave from FET 5 undergoes 20 ps relative phase delay (which is 72 degrees of a 10 GHz cycle) before combining with the the 10 GHz forward wave

[1] Kolner, B.H. and Bloom, D.M.: "Electro-Optic Sampling in GaAs Integrated Circuits", IEEE J. Quant. Elec., vol. -22, Jan. 1986, pp. 79-93.

[2] Weingarten, K.J., Rodwell, M.J.W., Heinrich, H.K., Kolner, B.H., and Bloom, D.M.: "Direct Electro-Optic Sampling of GaAs Integrated Circuits", Electron. Lett. 1985, *21*, pp. 765-766.

[3] Freeman, J.L., Diamond, S.K., Fong, H., and Bloom, D.M.: "Electro-optic sampling of planar digital integrated circuits", Appl. Phys. Lett., 1985, *47*, pp. 1083-1084.

[4] Valdmanis, J.A., Mourou, G.A., and Gabel, C.W.: "Subpicosecond Electrical Sampling" IEEE J. Quant. Elec., vol. *QE-19*, Apr. 1983, pp. 664-667.

[5] Beyer, J.B., Prasad, S.N., Becker, R.C., Nordman, J.E., and Hohenwarter, G.K.: "MESFET Distributed Amplifier Design Guidelines", IEEE Trans. MTT, vol. *MTT-32*, March 1984, pp. 268-275.

[6] Riaziat, M., Zubeck, I., Bandy, S., and Zdasuik, G.: "Coplanar Waveguides Used in 2-18 GHz Distributed Amplifier", ***to be published***, 1986 IEEE MTT-S International Microwave Symposium, Baltimore, MD.

[7] Ayasli, Y., Mozzi, R.L., Vorhaus, J.L., Reynolds, L.D., and Pucel, R.A.: "A Monolithic GaAs 1-13 GHz Traveling-Wave Amplifier" IEEE Tran. MTT. vol *MTT-30*, No. 7, July 1982, pp. 976-981.

[8] Ayasli, Y., Reynolds, L.D., Mozzi, R.L., and Hanes, L.K.: "2-20 GHz GaAs Traveling-Wave Power Amplifier" ibid., vol. MTT-32, no. 3, March 1984, pp. 290-295.

[9] Ladbrooke, P.H.: "Large-Signal Criteria for the Design of GaAs FET Distributed Power Amplifiers" IEEE Trans. on Electron Devices, vol. *ED-32*, no. 9, Sept. 1985, pp. 1745-1748.

Figure 1
Rodwell
et al

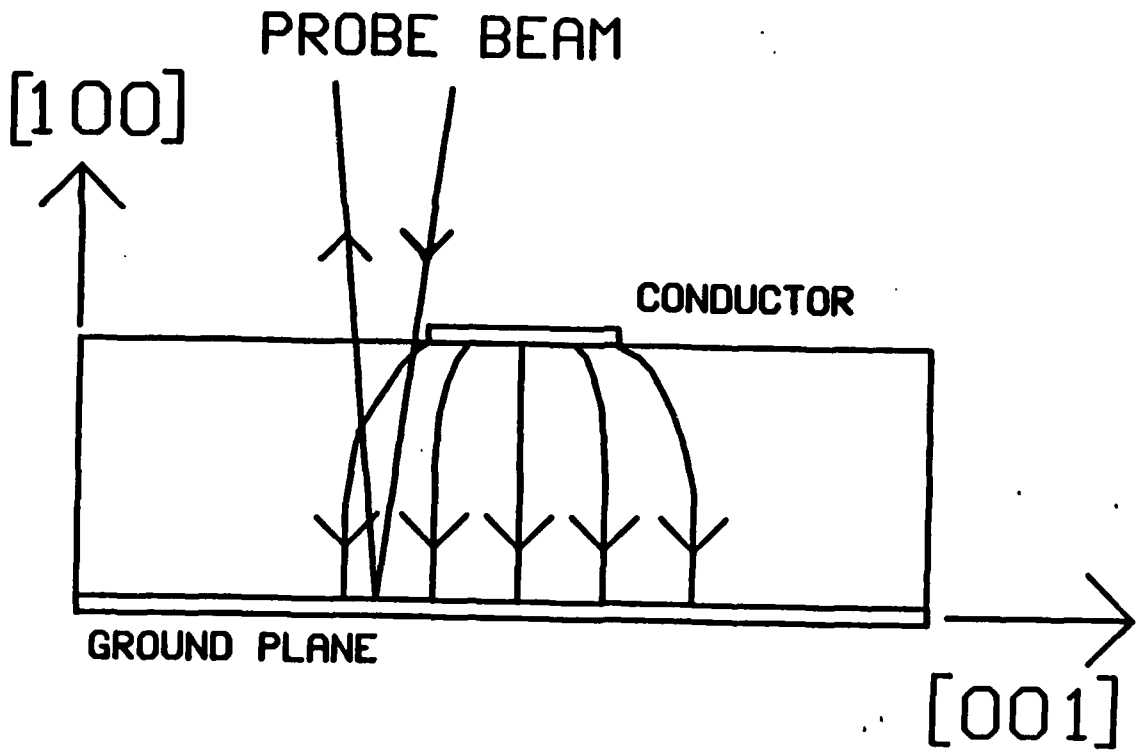

Figure 3
Rodwell
et al.

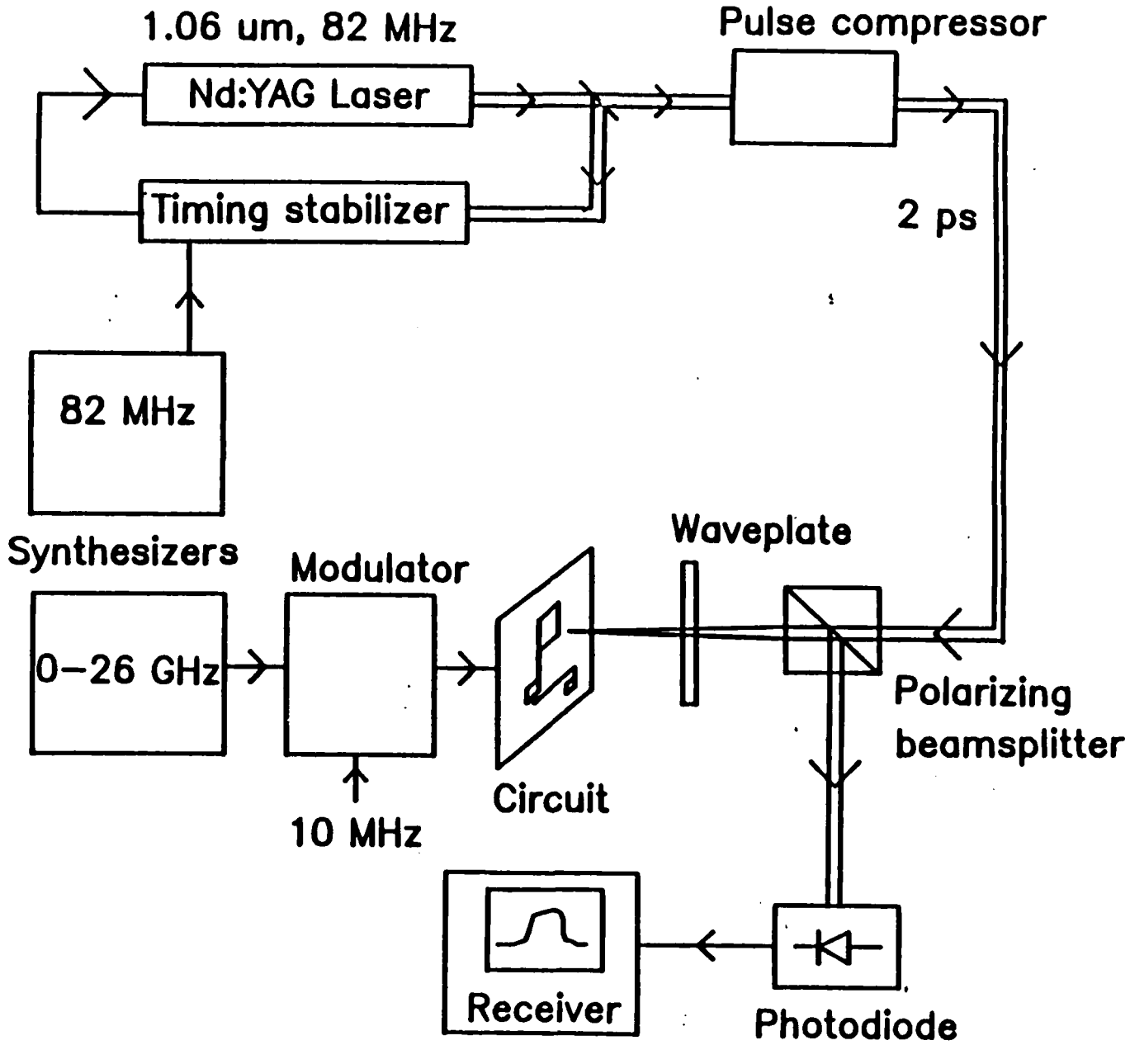

Figure 5
Rodwell et al

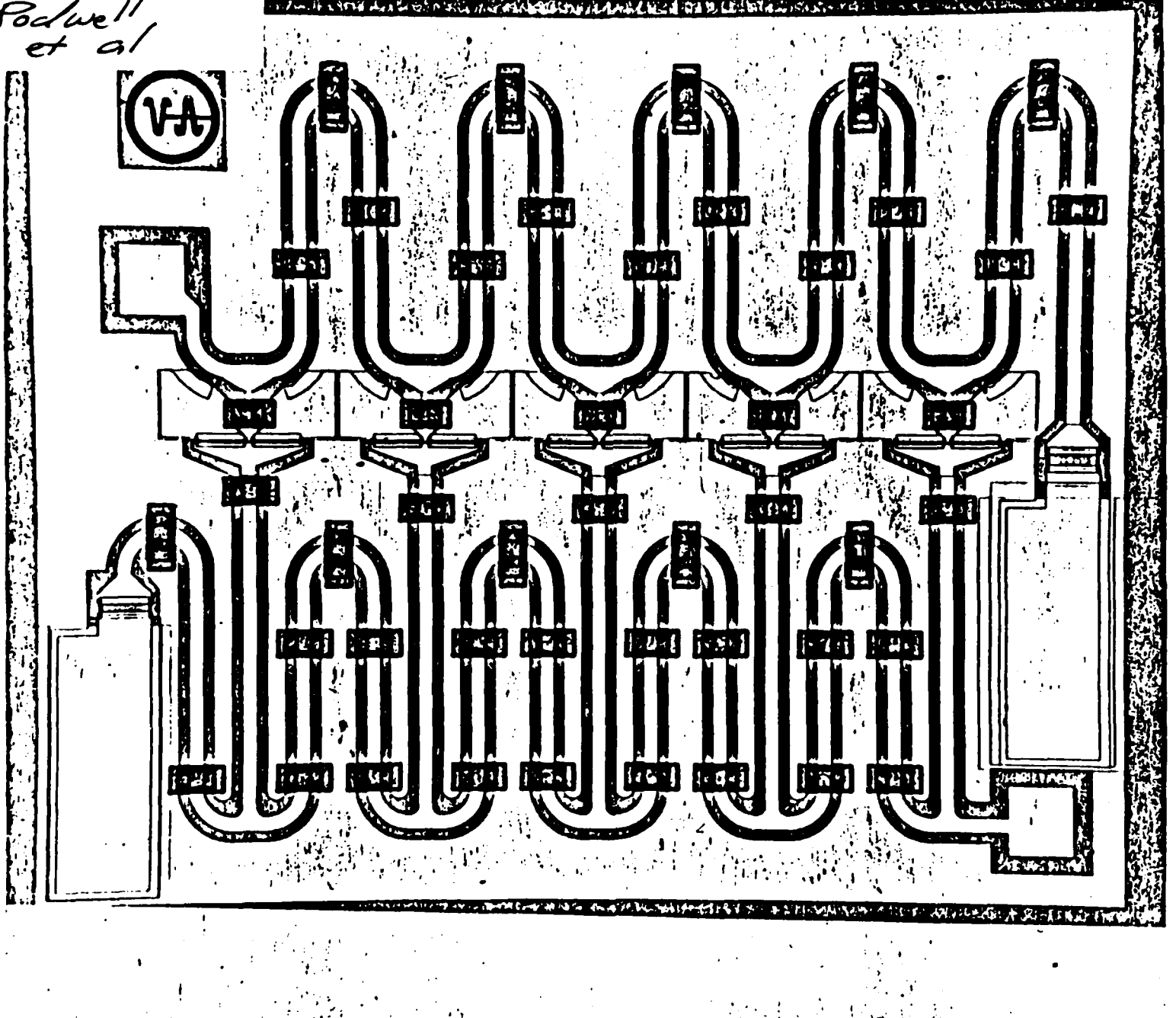

Figure 7
Rodwell
et al.

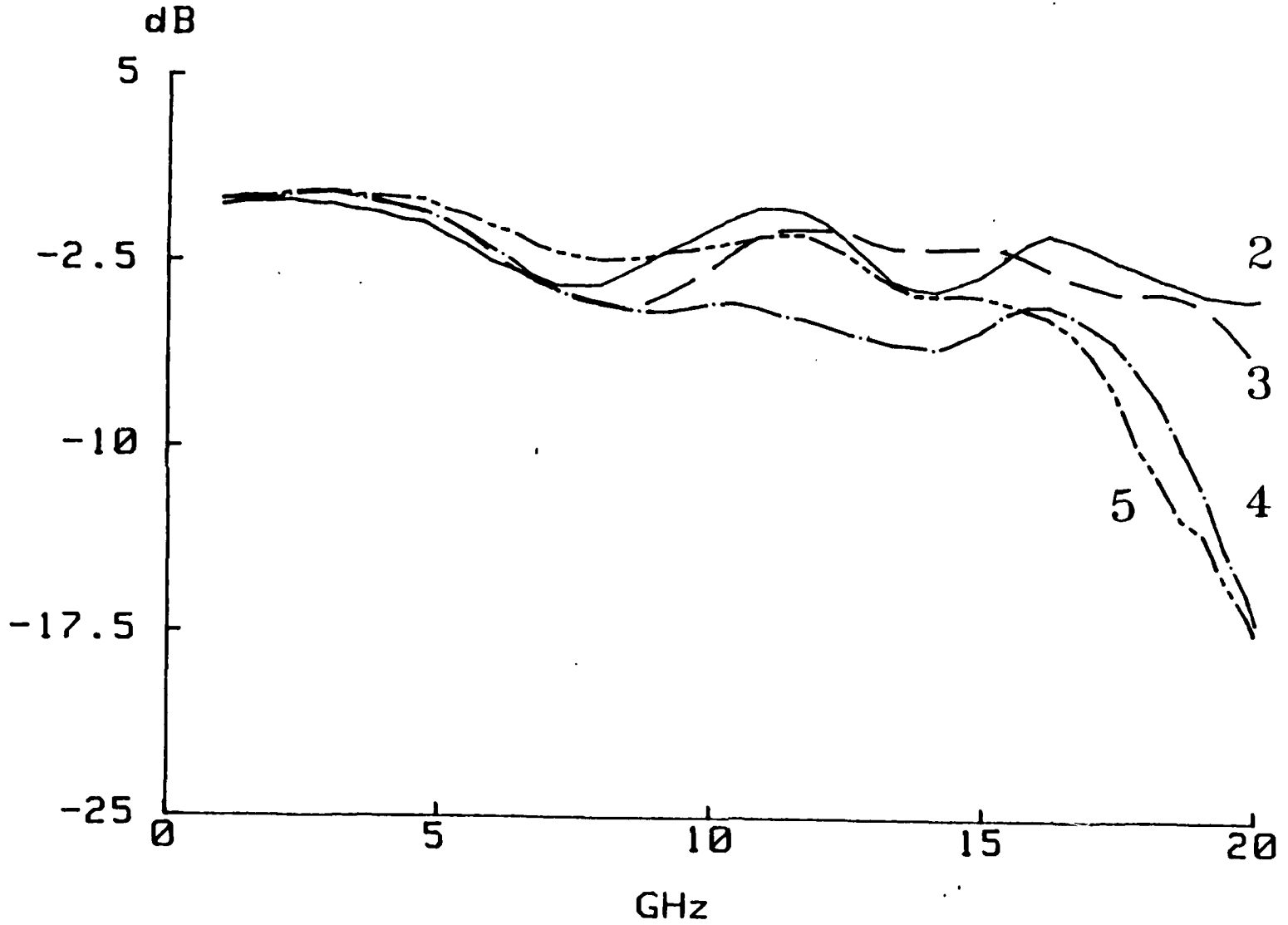

Figure 9
Rodwell
et al

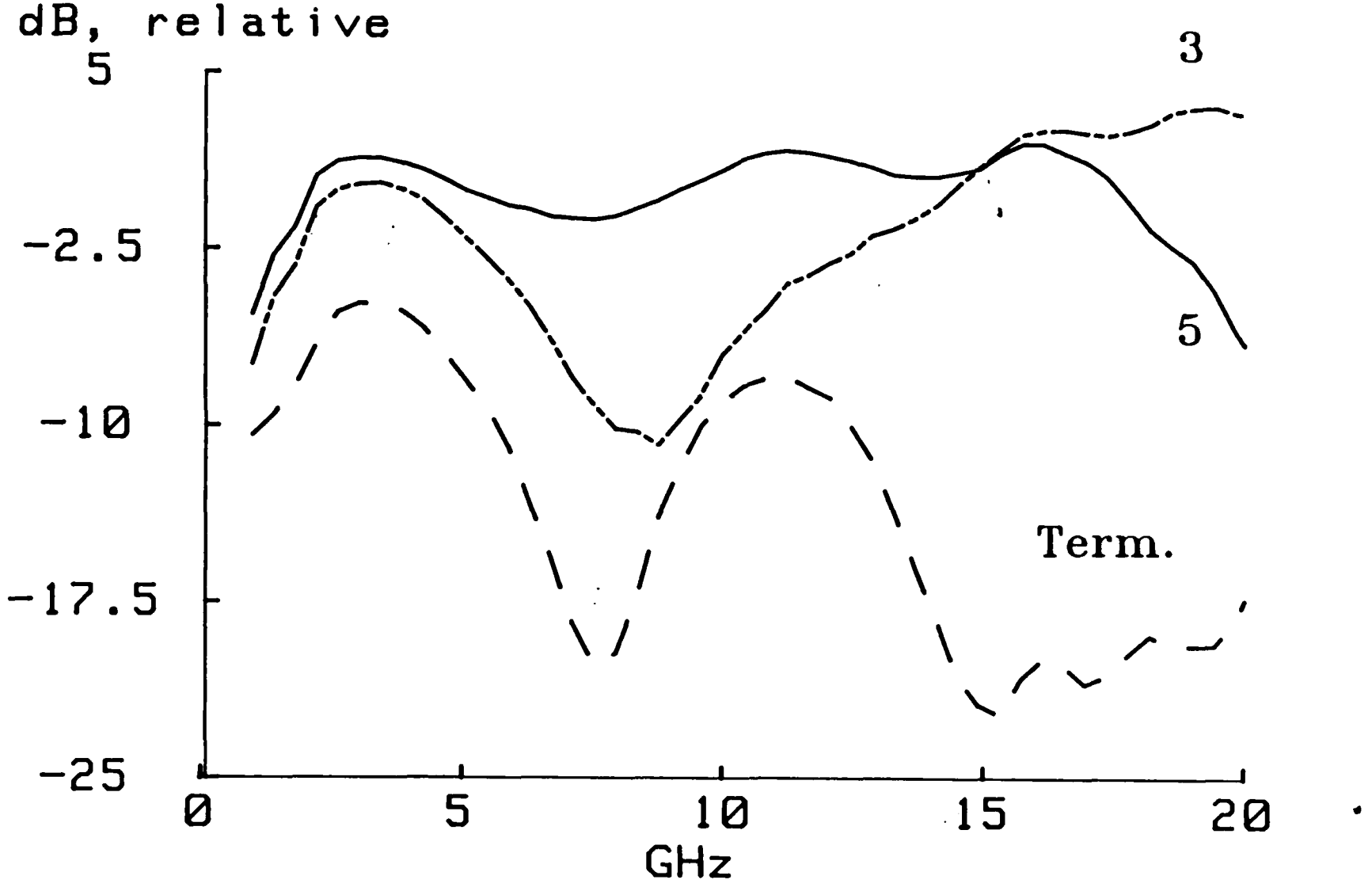

Figure 11
Rockwell
et al

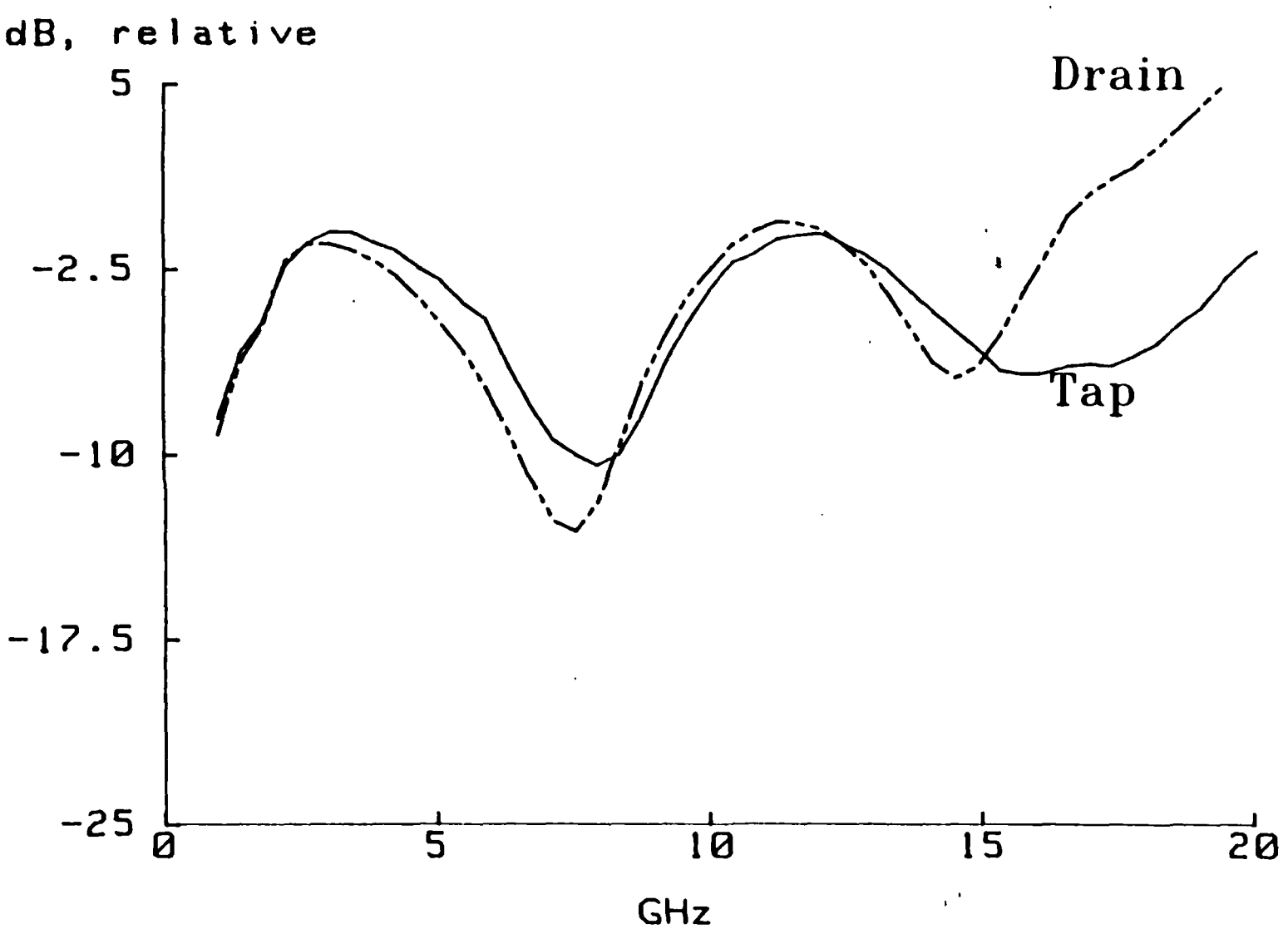

Figure 13
Rodwell et al

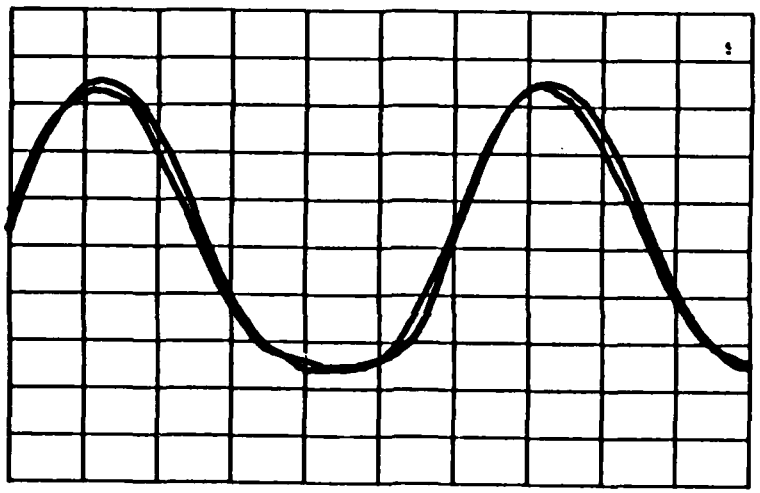

55 ps/div.

Figure 15
Rodwell et al

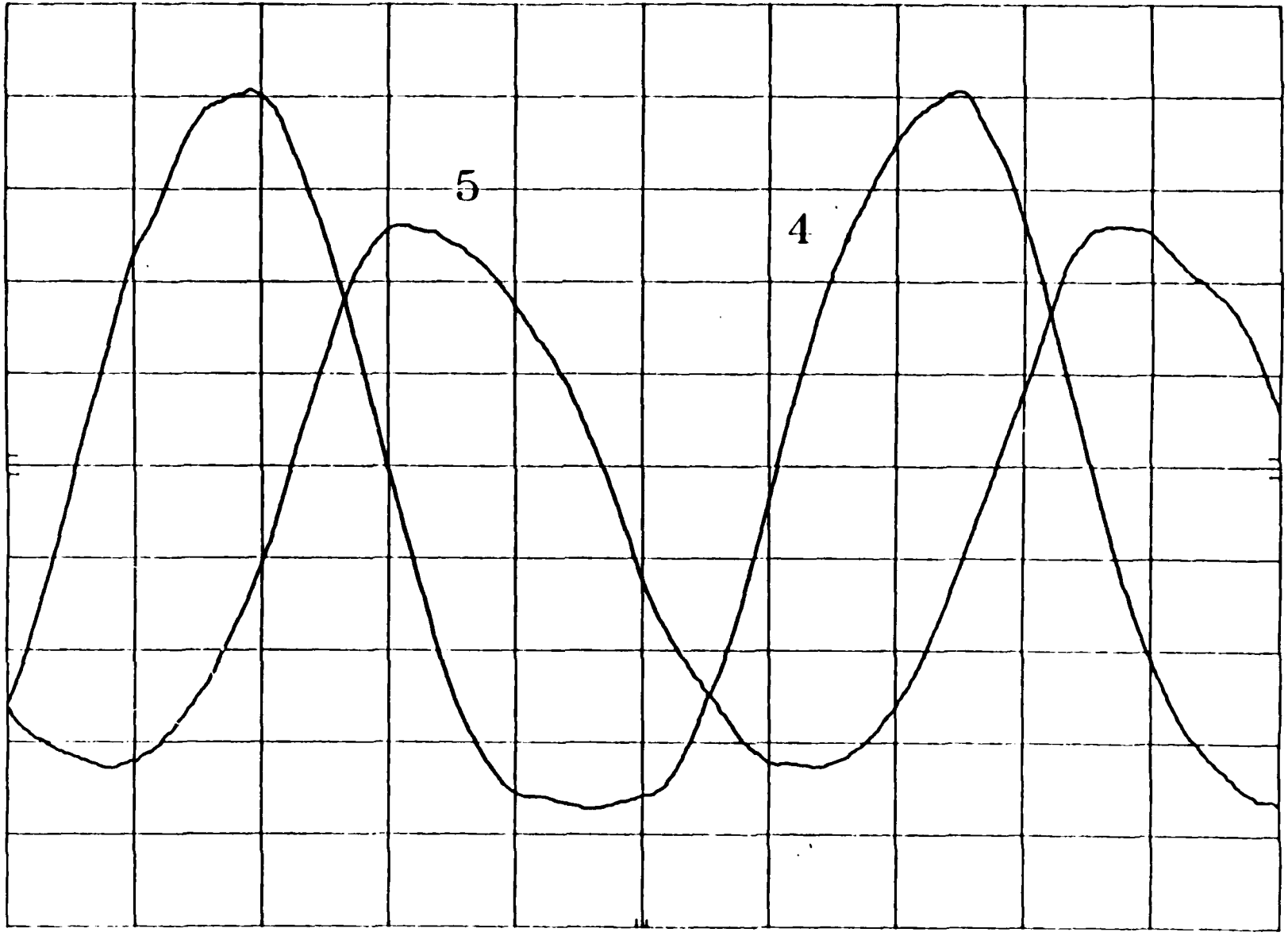

Electrooptic Sampling of Gallium Arsenide Integrated Circuits

K.J. Weingarten, M.J.W. Rodwell, J.L.Freeman,

S.K. Diamond, and D.M. Bloom

Edward L. Ginzton Laboratory

Stanford University

Stanford, CA 94305, USA

ABSTRACT

We report on electrooptic sampling with emphasis on measurements made directly to both analog and digital gallium arsenide integrated circuits to millimeter wave frequencies.

Invited Paper to the Topical Meeting on Ultrafast Phenomena, 1986

Electrooptic Sampling of GaAs Integrated Circuits

K.J. Weingarten, M.J.W. Rodwell, J.L. Freeman,
S.K. Diamond, and D.M. Bloom

Edward L. Ginzton Laboratory
Stanford University
Stanford, CA 94305, USA

Since its introduction [1], electrooptic (EO) sampling has rapidly developed as a tool for ultrafast electrical measurements [2], [3] with temporal resolution extending to less than a picosecond. The basic physical phenomenon underlying this technique, the Pockels effect, is well-described in the literature [1-5]. The work reported here relies on the fact that GaAs, the substrate material for many high-speed circuits, is electrooptic. Using a longitudinal probing geometry [4], [5], sub-bandgap energy infrared light is passed through the substrate of GaAs integrated circuits (IC's), reflected off some circuit metallization, and passed through a polarizer, resulting in an intensity change of the light proportional to the voltage across the substrate. In addition, the signal generating electronics for driving the IC's are phase locked to the repetition rate of a mode-locked laser laser, allowing sampled measurements of voltage waveforms due to sinusoidal excitation of the circuit. Figure 1 shows the system schematic.

This system can be used in several modes to make a variety of electrical measurements suitable for both analog and digital circuits. The EO effect acts like a mixer between the signal on the circuit and the fourier spectrum of the intensity envelope of the laser. A microwave or millimeter wave signal on the circuit mixes with the nearest laser harmonic signal to produce a low frequency IF whose the amplitude and phase can be readily measured. Thus high frequency vector measurements for linear network analysis can be made.

The sampling system also detects large signals, i.e. clipping and distortion, on analog circuits and switching waveforms on digital circuits. The timing stability of the laser with respect to the signal synthesizer is about 1 ps per minute, allowing for precise measurements of propagation delays through logic elements.

Results from a variety of analog and digital circuits will be presented, including measurements on broadband microwave amplifiers, signals to 40 GHz (the current limit of the microwave synthesizer) (Fig. 2), and timing/propagation delays for high-speed MESFETS (Fig. 3).

References

1. J.A. Valdmanis, G.A. Mourou, and C.W. Gabel, "Subpicosecond electrical sampling," IEEE J. Quant. Elec., vol QE-19, pp. 664-667, 1983.

2. B.H. Kolner and D.M. Bloom, "Electrooptic sampling in GaAs integrated circuits," IEEE J. Quant. Elec., vol. QE-22, pp. 79-93, 1986.

END

3-87

DTIC